

## FUNDAMENTAL ISSUES OF EARTH'S CRYOSPHERE

LATE QUATERNARY SAND COVERS  
OF CENTRAL YAKUTIA (EASTERN SIBERIA): STRUCTURE, FACIES COMPOSITION  
AND PALEOENVIRONMENT SIGNIFICANCE

A.A. Galanin

*Melnikov Permafrost Institute, Siberian Branch of the Russian Academy of Sciences,  
Merzlotnaya str. 36, Yakutsk, 677010, Russia; agalanin@gmail.com*

An additional comprehensive study of the Peschanaya Gora (Sand Hill) outcrop and other sections of aeolian coversands in Central Yakutia has revealed that, together with loess-ice (Yedoma) covers, they were two related granulometric and mineralogical derivatives which had formed as a result of aeolian processing of Quaternary alluvium during the second half of the Late Neopleistocene. Episodes of desertification took place 22.0–14.0, 12.8–11.8, and 0.6–0.1 ka BP. A decrease in aeolian activity and consolidation of dune massifs by a soil-vegetative cover took place in the intervals of 14.0–13.0 and 10.0–0.6 ka BP. The largest episode of desertification took place during the last global thermic minimum (MIS-2) and led to a sharp decline in the mammoth biome, the disappearance of the woolly mammoth and rhinoceros in Central Yakutia.

**Key words:** aeolian formation, D'olkuminskaya Series, cryogenic-aeolian, niveo-aeolian lamination, desertification, Late Pleistocene, Holocene, Bolling, Allerod, Younger Dryas, Eastern Siberia.

## INTRODUCTION

The studied region is located in the southern part of the Central Yakutian Lowland, within the Mesozoic Vilyuy Lowland of the Siberian platform. The sedimentary cover of the platform, which is exposed in the base of the Lena River's and its tributaries' high terraces, consists of Lower Paleozoic carbonate and Mesozoic-Cenozoic terrigenous deposits. Quaternary formations are represented by alluvial, lake, aeolian, and polygenic (cryogenic-aeolian) facies groups. The most abundant among them are Late Neopleistocene loess-ice deposits (Yedoma Series) with large polygonal ice wedges (PIW), as well as loess and sand covers and dune massifs (D'olkuminskaya Series) with a small ground ice content (Fig. 1, 2).

The climate of the region is sharply continental, with an average annual temperature of approximately  $-7^{\circ}\text{C}$ , annual precipitation varying from 140 to 250 mm, and a precipitation-evaporation ratio of 0.8–1.0. Permafrost 200–600 m thick with a temperature of  $-3$  to  $-7^{\circ}\text{C}$  is distributed throughout the region. The thickness of the active layer varies from 0.5 to 2.5 m [Ershov, 1989].

Various types of larch forests (*Larix gmelinii*) dominate the region's vegetation cover, with a mixture of pine (*Pinus sylvestris*), spruce (*Picea obovata*), and birch trees (*Betula platyphylla*, *B. pendula*). Shrub birches (*Betula exilis*, *B. nana*), alder elfin (*Alnus fruticosa*), the genus *Rosa* (*Rosaceae* sp.) dominate the canopy layer; subshrub heath (*Ericaceae*

fam.), spike moss (*Selaginella rupestris*), creeping cedars (*Lycopodium annotinum*, *L. pungens*, *L. clavatum*, etc.), mosses (Bryophyta), fructicose lichens (*Cladina* sp., *Cetraria* sp., etc.) dominate the ground layer. Grasses, sedges, and Asteraceae (Poaceae fam., Cyperaceae and Asteraceae) dominate the herbaceous layer [Kuznetsova et al., 2010].

Forestless landscapes are distributed fragmentarily on floodplains, low terraces, alas basins, and on steep slopes with a southern aspect. They are represented by meadow, steppe, and semi-desert herbaceous groupings consisting of feather grass (*Stipa capillata*), fescue (*Festuca lenensis*), Kobresia (*Kobresia filifolia*), sedges (*Carex duriuscula*, *C. pediformis*), wheatgrass (*Elytrigia jacutorum*), sagebrush (*Artemisia frigida*, *A. tanacetifolia*, *A. karavajevii*), buttercup (*Anemone sylvestris*), etc. Halophytic species are common (*Goniolimon speciosum*, *Salicornia europaea*, etc.).

Semi-desert groups are more common within modern dune massifs (Tukulans). The extremely sparse vegetation cover is formed by single curtains of xerophytic semi-subshrubs (*Thymus sergievskajae*, *Krascheninnikovia lenensis*, *Ephedra monosperma*) and perennial grasses, many of which are endemic (*Koeleria skrjabinii*, *K. karavajevii*, *Artemisia karavajevii*, *Phlojodicarpus sibiricus*, *Rumex graminifolius*, etc.).

The Peschanaya Gora outcrop ( $62^{\circ}88.21' \text{N}$ ,  $129^{\circ}80.68' \text{E}$ ), also called Shishkinskiy Yar and D'olkuma-Khayata (as cited in [Kamaletdinov, Minuk,

1991]), is located on the right bank of the Lena River, 100 km north of Yakutsk (Fig. 1), and is one of the key sections of cover dune deposits of Central Yakutia. The cross- and wavy-stratification sands (up to 20 m thick) which emerge in the 18–25 m cliff of the (Kerdyom) terrace were named the D'olkuminskaya Series and dated to the last MIS-2 (marine isotope stage) cryochrone of the Late Neopleistocene [Kolpakov, 1983; Alekseev et al., 1984, 1990; Kamaletdinov, Minuk, 1991]. The relatively young age of the D'Olukuminskaya Series is evidenced by its top, which is clearly expressed in the modern relief as vegetated U-shaped and longitudinal dunes with a southeast axis orientation (Fig. 2, a, b). Individual dunes reach a length of 2 km, a width of 300–400 m, and a height of 10–15 m.

Aeolian cover sands similar in composition, structure and age are known in many cold regions of

Northern Eurasia: Transbaikalia and Baikalia [Ivanov, 1966; Ufimtsev et al., 1997; Vyrkin, 2010], Western Siberia [Volkov, 1971; Fedorovich, 1983; Velichko, Timireva, 2005; Sizov, 2015; Zykina et al., 2017; Konstantinov et al., 2019; Sizov et al., 2020], Northern Europe [Schwan, 1986, 1988; Kasse, 2002; Astakhov, Svensen, 2011], and also in Alaska and Canada [Black, 1951; Pewe, 1975; Carter, 1981; Koster, Dijkmans, 1988; Lea, 1996; Wolfe et al., 2011].

In 1984 the Peschanaya Gora outcrop was added to the list of unique objects in the scientific excursion of the 27<sup>th</sup> International Geological Congress that took place in Yakutsk [Alekseev et al., 1984]. Later, D'olkuminskaya Series deposits were documented in different volumes in the structure of both the low and the highest terraces of the Lena River (Fig. 1) [Kamaletdinov, Minuk, 1991; Waters et al., 1999; Bolshiyakov et al., 2016; Spektor et al., 2016, 2017; Pravkin et

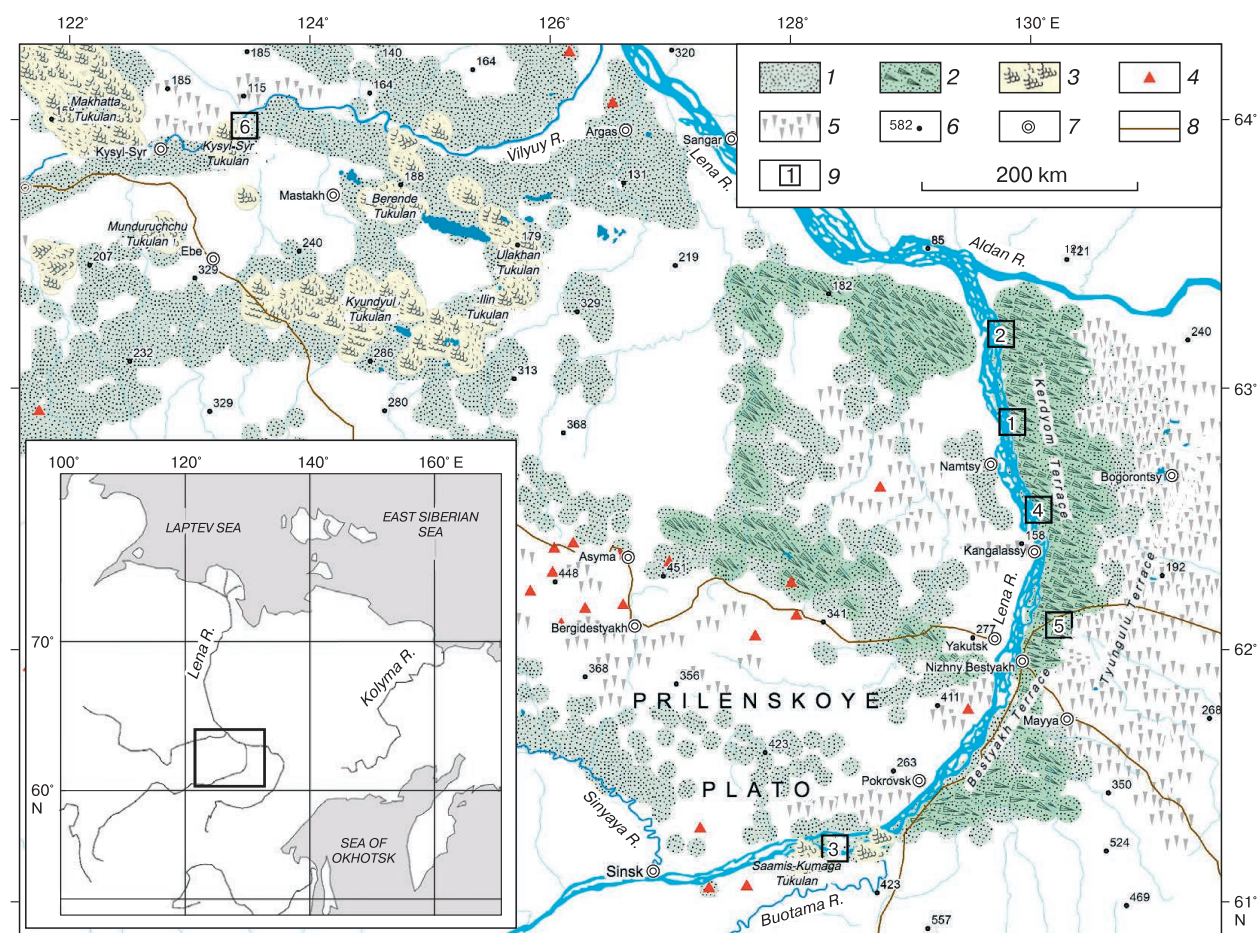


**Fig. 1. Distribution of D'olkuminskaya Series cover aeolian deposits and modern unfixed dune massifs (Tukulans) in Central Yakutia.**

1 – fixed sand covers of the last glacial maximum (MIS-2); 2 – fixed U-shaped and longitudinal dunes of the Younger Dryas; 3 – unfixed parabolic dunes (Tukulans) of the Little Ice Age; 4 – findings of large accumulations of ventifacts; 5 – accumulative plains and plateaus with Yedoma Series Late Neopleistocene ice-loess covers (MIS-3–MIS-2); 6 – height markers; 7 – populated areas; 8 – roads; 9 – D'olkuminskaya Series key sections discussed in the present article: 1 – Peschanaya Gora; 2 – Kharyyalakh; 3 – Ust'-Buotama; 4 – Suullar Myraan; 5 – Megin; 6 – Kysyl-Syr.



**Fig. 2. Some forms of the aeolian and cryogenic-aeolian relief of Central Yakutia, composed of sand and loess-ice cover deposits of the second half of the Late Neopleistocene.**

*a, b* – fixed U-shaped dunes on the surface of the 18–25-meter Kerdymom (*a*) and 45–75-meter Bestyakh (*b*) terraces of the Lena River in the territory surrounding Yakutsk; *c* – modern embryonic parabolic dune on the surface of the 30-meter terrace of the Vilyuy River; *d* – large modern dune massif (Tukulan), which intersects various elements of the Vilyuy River valley; *e* – modern dune massif (Ilin Tukulan) which partially blocks the Lungkha River valley (right tributary of the Vilyuy); *f* – 30-meter-tall cover dune on the brink of the Bestyakh terrace of the Lena River; *g* – thermodenudational relief within the distribution of ice-loess deposits of the Yedoma Series of the 75–150-meter (Tyungulu) terrace of the Lena River; *h* – Muus Appa deflational ventifact plateau within the Lena-Vilyuy drainage divide. Fig. 2, *a, b, g, h* – satellite images from the portal Yandex.Maps. Fig. 2, *c, d, e, f* – A.A. Galanin's photo from July–August 2019.

*al., 2018*], in the basin of the lower course of the Vilyuy River [*Galanin et al., 2016, 2018; Galanin, Pavlova, 2019*], and also identified in the terminal Middle and Late Neopleistocene moraines of the Verkhoyansk glaciers [*Siegert et al., 2007*]. The maximum thickness of the series (more than 70 m) is seen in the Ust'-Buotama outcrop of the Bestyakh terrace of the Lena River, 120 km south of Yakutsk.

To this day a fairly large amount of radiocarbon and optical luminescence (OSL) dates falling within

the range of 30 to 10 ka has been obtained from D'olkuminskaya Series deposits, which indicates the series' formation over the course of MIS-2 in the last cryochrome [*Galanin, Pavlova, 2019*].

Numerous lithological and structural features indicate an aeolian origin of the D'olkuminskaya Series [*Kolpakov, 1983; Pewe, Journaux, 1983; Kamaltdinov, Minuk, 1991; Waters et al., 1999; Siegert et al., 2007; Galanin et al., 2018*]. Aeolian genesis is also evidenced by a mantle-like bedding, the distribution

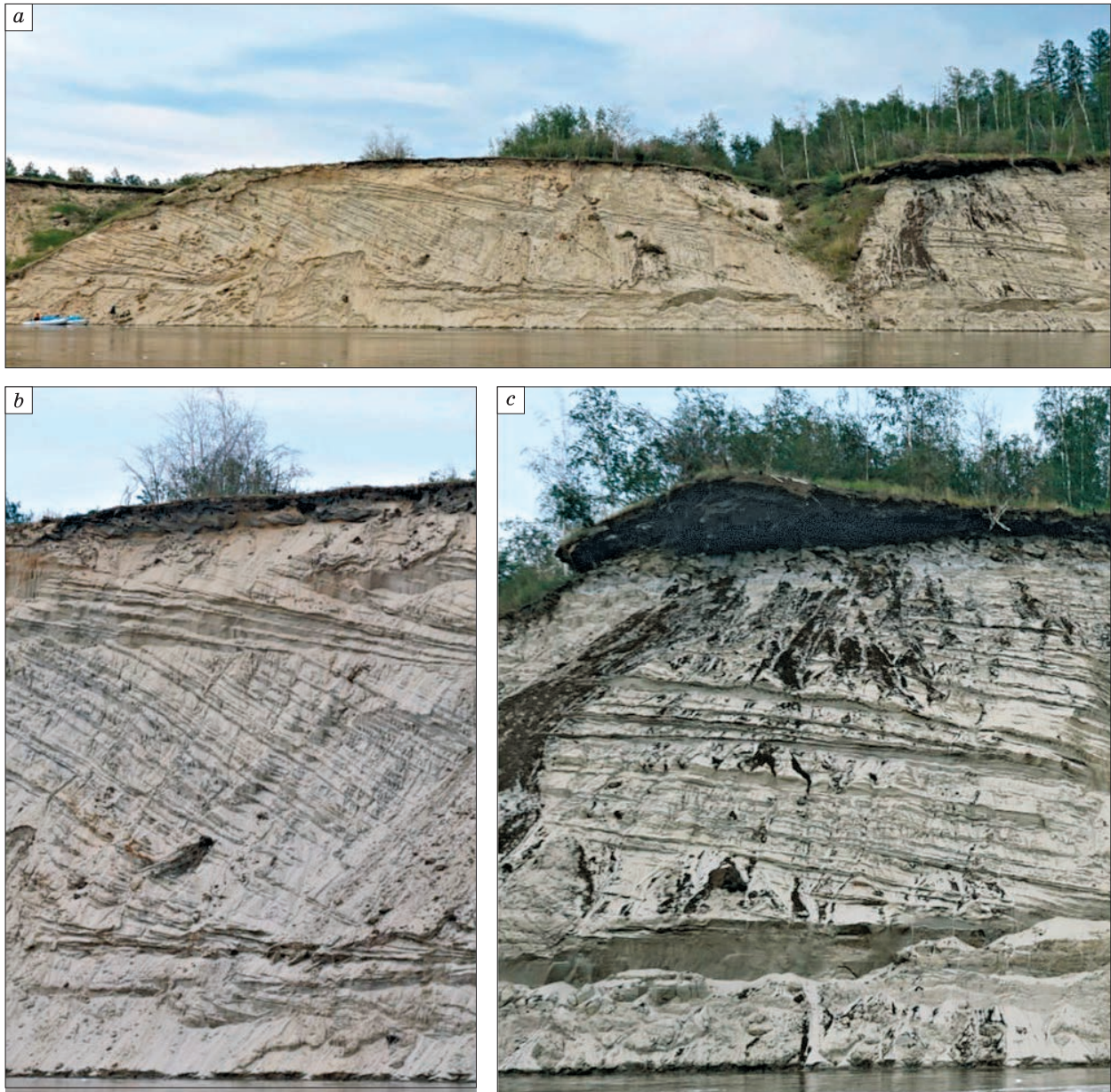


**Fig. 3. Key outcrop Peschanaya Gora in the escarpment of the 18–25-meter (Kerdyom) terrace of the Lena River.**

High overflow of the Lena River in August 2018 exposed expressive inclined, diagonal and cross-bedded D'olkuminskaya Series stratification types. *a* – overall appearance of the studied area; *b* – cross-bedded macrostructure of dune sands; *c* – Holocene peat bog in the roof of the D'olkuminskaya Series. A.A. Galanin's photo from August, 2019.

of sand covers across different hypsometric levels (Fig. 1), including watersheds, and the xerothermic composition of fossilized flora and fauna, in which cold steppe and desert taxa dominate [Kolpakov, 1983; Kamaletdinov, Minuk, 1991; Filippov, Vasiliev, 2006; Galanin, Pavlova, 2019].

Holocene and modern unvegetated dune massifs called Tukulans are widespread in the region in association with Late Neopleistocene D'olkuminskaya Series sand covers (Fig. 2, c–f). Their total area exceeds 3,000 km<sup>2</sup> [Galanin et al., 2016; Galanin, Pavlova, 2019]. The bigger ones – the Makhatta, Ulakhan, Kysyl-Syr, and other Tukulans – are located in the basin of the lower course of the Vilyuy River. The Saamis-Kumaga and Lenskaya Dune Tukulans, which model the surface of the 75–100-m (Bestyakh) terrace of the Lena River in the vicinity of the Ust'-Buotama outcrop and are comprised of unvegetated parabolic dunes up to 30 m in height (Fig. 2, f), are known in the territory surrounding Yakutsk.

For a long time the D'olkuminskaya Series was presented on geological maps as river and lake deposits [Map..., 1959; Map..., 1983]. It was assumed that cover sands were a particular type of “periglacial alluvium” and the dunes that lie atop the surface of the terraces had formed as a result of its wind reworking [Soloviev, 1959; Alekseev, 1961]. The lengthy denial of aeolian genesis of the D'olkuminskaya Series is also due to a lack of confidence in the existence of mixed-age river terraces in the Lena River Basin in this case, and the principle of distinguishing them by relative height is broken altogether.

Despite the appearance of Late Neopleistocene dune covers on the new geological map [Map..., 2014], the structure of the key outcrop Peschanaya Gora, the distribution areas, and the genesis of the D'olkuminskaya Series are currently under discussion. Some researchers are attempting to explain the series' “gigantic inclined and wavy stratification which has no modern analogues” (Fig. 3) using the activity of catastrophic floods and spillways moving transversely across the valley of the Lena River [Spektor et al., 2016, 2017]. Another group of authors [Bolshiyarov et al., 2013, 2016; Pomortsev et al., 2017] ties the origin of sand covers to a rise in the level of the Lena River by 100–150 m during MIS-3 as a result of “a change in the base of erosion and backwater from the sea” [Pravkin et al., 2018, p. 225].

Various types of stratification and lamination, the taxonomy and origin of which are poorly studied, are common in D'olkuminskaya Series deposits. The diagonal and gigantic oblique types of stratification (Fig. 3), referred to by some researchers as alluvial oblique stratification, are of particular importance. It was supposed for a long time that its formation is related to the unusual regimes of Late Neopleistocene watercourses and particular facies of “periglacial al-

luvium,” modern analogues of which do not exist [Soloviev, 1959; Alekseev, 1961; Ershov, 1989; Bolshiyarov et al., 2016; Spektor et al., 2016, 2017; Pravkin et al., 2018]. Discussions arise not only from the unusual types of stratification and lamination, but also from the ubiquitous southeast strike of the strata. It completely diverges from the direction of the flow of modern rivers, but matches the southeast orientation of the dune relief on the surface of river terraces and corresponds to the main direction of atmospheric transport in the region (Fig. 1, 2, a, b).

In 2017–2020 the authors of the present article conducted an additional study of the structure and granulometric and mineralogical composition of Peschanaya Gora deposits and obtained new radiocarbon dates. Special attention was paid to the study of the structure of the deposits (stratification and lamination).

The goal of the present article is to provide a more complete description of the Peschanaya Gora outcrop and to discuss, taking into account both new data and data published earlier, the main features of the structure and origin of D'olkuminskaya Series deposits and the Late Quaternary relief of Central Yakutia and Eastern Siberia.

## RESEARCH MATERIALS AND METHODS

The factual material of the present article is based on the study of natural outcrops using standard methods of Quaternary geology, geomorphology, structural and facies analyses.

The granulometric analysis (42 samples) was completed in accordance with GOST 12536-2014 [2015] methods of sieving and areometry in the Melnikov Permafrost Institute (MPI), SB RAS granulometric laboratory. V.V. Okhotin's [1933] granulometric classification denominations were used to describe deposits. Statistical processing of the results was completed in the Gradstat program [Blott, Pye, 2001] using the modified geometric method [Folk, 1980; Blott, Pye, 2001]. Mean ( $x$ ) and median (Md) grain sizes were calculated in micrometres ( $\mu\text{m}$ ); other values – grain sorting coefficient ( $\sigma$ ), skewness (asymmetry) ( $\alpha$ ), and excess kurtosis ( $\tau$ ) – were calculated in dimensionless units of logarithmic scale [Blott, Pye, 2001]. The results of the analysis are shown in Table 1.

The quantitative immersion mineralogical analysis (28 samples) was completed in the MPI SB RAS laboratory using binocular and polarizing mineralogical microscopes, as well as immersion liquids. Mineral grain count was completed simultaneously for two fractions: 100–50  $\mu\text{m}$  and 50–10  $\mu\text{m}$ . 300–350 grains were taken from each sample and fraction from a random batch, based on which the percentage content of each mineral was calculated. The results of the mineralogical analysis are shown in Table 2.

Table 1. **Granulometric composition of the deposits of the 18–15-meter terrace of the Lena River in the Peschanaya Gora outcrop (Central Yakutia)**

Deposit unit number	Interval (m)	Number of samples	$x$ , $\mu\text{m}$	$\sigma$	$\alpha$	$\tau$	Md, $\mu\text{m}$
Ia	0–2.45	8	$316.8 \pm 64.9$	$2.03 \pm 0.16$	$0.04 \pm 0.10$	$1.10 \pm 0.18$	$317.8 \pm 63.5$
Ib	2.45–2.50	2	$56.2 \pm 1.1$	$4.43 \pm 0.80$	$-0.25 \pm 0.15$	$0.85 \pm 0.03$	$71.7 \pm 11.5$
IIb	5.0–7.0	2	$253.9 \pm 10.9$	$1.84 \pm 0.16$	$-0.06 \pm 0.02$	$0.82 \pm 0.06$	$260.9 \pm 7.1$
IIIa	10.0–17.0	2	$298.4 \pm 79.5$	$1.70 \pm 0.04$	$0.02 \pm 0.01$	$1.12 \pm 0.36$	$290.3 \pm 73.1$
IIIb	17.0–17.4	2	$649.0 \pm 331.8$	$1.71 \pm 0.23$	$-0.39 \pm 0.10$	$1.23 \pm 0.06$	$741.2 \pm 411.7$
IIIc	17.4–20.0	8	$240.2 \pm 17.0$	$1.69 \pm 0.06$	$-0.16 \pm 0.07$	$0.81 \pm 0.07$	$253.7 \pm 24.0$
IVa	20.0–20.4	1	44.5	4.29	0.13	0.95	38.0
IVb	20.4–22.4	4	$316.9 \pm 30.7$	$1.67 \pm 0.16$	$-0.21 \pm 0.07$	$1.18 \pm 0.15$	$334.4 \pm 18.6$

Note:  $x$  – mean grain size;  $\sigma$  – grain sorting coefficient;  $\alpha$  – skewness;  $\tau$  – excess kurtosis; Md – median.

Table 2. **Mineralogical composition of alluvial and aeolian sands in the 18–25-meter (Kerdyom) terrace of the Lena River in the Peschanaya Gora outcrop (Central Yakutia)**

Parameter		Unit number				
		I	II	IIIa	IIIc	
Sampling interval*, m		0–2.45	2.50–9.95	10.0–17.0	17.0–22.5	
Number of samples in fractions: 100–50 $\mu\text{m}$ ; 50–10 $\mu\text{m}$		6; 4	11; 5	5; 4	6; 2	
Minerals	Fraction, $\mu\text{m}$	Grain content in sample**, %				
Primary	Quartz	100–50	17.4–55.1; 39.9	25.1–50.8; 44.2	42.3–50.4; 47.4	43.9–56.2; 50.7
		50–10	8.5–27.2; 18.8	22.0–43.3; 34.3	33.8–56.0; 46.0	36.0–46.8; 41.4
	Feldspars	100–50	9.0–40.4; 28.1	17.7–44.9; 36.8	28.1–39.6; 35.1	33.4–43.7; 38.8
		50–10	6.7–16.2; 11.1	19.0–37.9; 29.0	17.0–44.1; 34.0	41.8–44.2; 43.0
Carbonates	100–50	1.4–68.4; 20.3	0.7–54.2; 9.7	0.9–11.7; 4.0	0.0–4.8; 0.9	
	50–10	16.6–80.0; 46.6	16.6–54.9; 27.6	2.1–24.3; 8.3	0.0–10.5; 5.3	
Amphiboles	100–50	1.5–13.2; 7.4	1.6–9.8; 5.3	2.5–7.3; 5.1	3.1–8.4; 5.6	
Secondary and accessory	Epidote	100–50	0.0–3.5; 0.8	0.0–3.8; 1.4	0.0–1.7; 0.6	0.0–3.4; 1.3
	Magnetite	100–50	0.0–1.9; 1.0	0.0–2.7; 1.1	0.0–4.8; 3.1	0.6–2.7; 1.7
	Biotite	100–50	0.0–1.1; 0.6	0.0–1.1; 0.2	0.0–0.6; 0.1	0.0–0.7; 0.2
		50–10	1.2–8.2; 4.2	1.6–5.7; 3.8	1.3–4.6; 2.4	3.2–4.1; 3.6
	Zircon	100–50	0.0–1.5; 0.6	0.0–1.4; 0.4	0.0–2.8; 0.8	0.0–0.7; 0.2
	Pyroxenes	100–50	0.0–1.2; 0.2	0.0–0.6; 0.2	0.0–0.6; 0.3	0.0–0.9; 0.2
	Chlorite	100–50	0.0–0.8; 0.3	single	0.0–0.6; 0.2	single
		50–10	0.0–3.0; 1.3	0.6–6.5; 2.6	0.0–1.8; 0.8	1.2–4.9; 3.1
	Garnet	100–50	0.0–1.3; 0.5	0.0–1.4; 0.3	none	0.0–0.5; 0.2
	Apatite	100–50	single	none	none	none
	Rutile	100–50	single	none	none	none
	Iron hydroxides	100–50	0.0–0.6; 0.1	0.0–0.5; 0.1	0.0–0.3; 0.1	0.0–0.3; 0.1
	Charcoal	100–50	0.5–1.5; 0.9	0.0–0.6; 0.5	0.0–11.7; 3.0	0.0–0.3; 0.1
50–10		0.6–18.4; 6.7	1.0–4.5; 2.8	1.6–18.4; 7.7	0.0–3.5; 1.8	

\* Sampling interval bottom-up.

\*\* Minimum and maximum values; mean.

**Radiocarbon dating** was completed in the MPI SB RAS radiocarbon laboratory (Yakutsk) using liquid scintillation counting on the Quantulus 1220 spectrometer-radiometer. Radiocarbon date calibration was completed using the OxCal 4.3 program for a 95 % level of significance [Bronk, 2009]. A portion of

the cited dates, which had been obtained by predecessors before the mid-1990s, was published earlier without calibration. Consequently, for ease of interpretation all such dates were also calibrated and rewritten using calendar age. Radiocarbon dates are shown in Table 3.

Table 3. Radiocarbon dates of the deposits in the 18-25-meter (Kerdyom) terrace of the Lena River in the Peschanaya Gora outcrop (Central Yakutia)

Unit number	Dating laboratory number	Height from baseflow edge of Lena River, m	Deposit type, dated material	<sup>14</sup> C age, y.a.	Calendar age*, y.a.	Cited reference
IVc	MPI-120	24.0	Paleosol, peat	6400 ± 300	7860–6650	Author's details
	MPI-119	23.5	Same	9500 ± 350	12 030–9890	Same
	MPI-118	23.0	Paleosol, shrub branches	6560 ± 350	8060–6720	Same
	GIN-2462	22.6	Paleosol, peat	7920 ± 60	8990–8600	[Alekseev et al., 1984, 1990]
	MPI-121	22.5	Same	8280 ± 250	9890–8580	Author's details
IIIb	GIN-2461	17.0	Same	11 850 ± 150	14 070–13 400	[Kamaletdinov, Minuk, 1991]
IIIa	MPI-760	11.0	Same	14 000 ± 500	18 330–15 680	[Alekseev et al., 1984, 1990]
	MPI-901	10.0	Paleosol, peat	14 450 ± 320	18 390–16 700	[Kamaletdinov, Minuk, 1991]
IIa	MPI-759	5.0	Alluvial vegetation detritus	17 200 ± 500	22 100–19 600	[Alekseev et al., 1984, 1990]

\* Interval with  $p > 94.9\%$  level of significance.

Stratification and lamination analysis of sediments was completed with consideration of the modern understanding of aeolian deposition mechanisms in cold regions, which were examined in detail in the works of R.E. Hunter and his followers [Hunter, 1977; Schwan, 1986, 1988; Kasse, 2002; Brookfield, 2011; Zieliński et al., 2015; Derbyshire, Owen, 2017; Kasse, Aalbersberg, 2019].

A large variety of geometric and genetic types of stratification and lamination of cold region dune deposits has been described to this day. Some of them are seen in both aeolian and alluvial deposits. However, there are specific types of lamination that are typical only for aeolian sands. Among them are *translatent climbing ripple lamination*, *grain-fall lamination* and *sandflow lamination*, which are typical for the steep leeward dune slope facies [Hunter, 1977; Brookfield, 2011]. Some aeolian and alluvio-aeolian deposit facies demonstrate a wide distribution of *adhesion lamination*, the formation of which is related to aeolian deposition onto a humid sedimentation surface. *Planebed*, *crinkly parallel* types, including *adhesion ripple lamination* and others, are common among adhesive structures [Hunter, 1977; Brookfield, 2011; Caputo, 2020].

Modern aeolian deposits of cold regions frequently have interbedded snow and ice layers which are buried under layers of sand and dust. Such deposits are described in modern Antarctic dunes, in Alaska within the Kobuk dune massif, and are called *niveo-aeolian* [Cailleux, 1974; Calkin, Rutherford, 1974; Koster, Dijkmans, 1988; Brookfield, 2011]. Numerous signs of syngenetic freezing and subsequent melting were identified in European, Canadian, and Alaskan cover aeolian deposits which had formed at the end of the Late Neopleistocene in the interval of 14.0–12.5 ka [Koster, Dijkmans, 1988; Kasse, 2002; Brook-

field, 2011; Zieliński et al., 2015; Derbyshire, Owen, 2017; Kasse, Aalbersberg, 2019]. Structures related to the melting of buried snow and ice are called *denivation structures* and play a very significant role in facies analysis of aeolian deposits of cold regions [Dijkmans et al., 1986; Koster, Dijkmans, 1988; Brookfield, 2011].

#### Structure and facies composition of the key outcrop Peschanaya Gora

The Peschanaya Gora outcrop is located on the right bank of the Lena River, 60 km upstream of the Aldan River mouth and 14 km northeast of the small town of Grafskiy Bereg. Here, in the river cliff of the 18–25 m (Kerdyom) terrace (approximately 7 km long), the D'olkuminskaya Series structure is exposed (Fig. 3). The surface of the terrace is covered with parallel rows of U-shaped dunes (Fig. 2, a) with a southeast axis orientation (110–130° azimuth). The length of individual dunes varies from 500 m to 3 km, their width varies from 50 to 200 m, the maximum height of the dune brinks above the interdune basins is 5–10 m. A pine forest covers the dune brinks, and groups of birches, creeping shrub-sedge thickets, meadows, swamps, and small peat bogs and lakes are common in the interdune depressions. In the north part of the outcrop (62°88.21' N, 129°80.68' E), from the Lena River baseflow level up, the following stratigraphic units were highlighted in the R-537 section (Fig. 4).

**Unit Ia (0.0–2.45 m)** is composed of horizontally interlayering series of gravelly coarse sands, fine sands, and loamy sands with a mix of pebbles of local (limestone, dolomite) and distant transportation (gneisses, granitoids, quartzites, vulcanites, etc.). The color of the sediments varies from light-yellow to reddish-brown, occasionally intensely ochre. There are bright ochre-colored sand-loam crusts and lenses

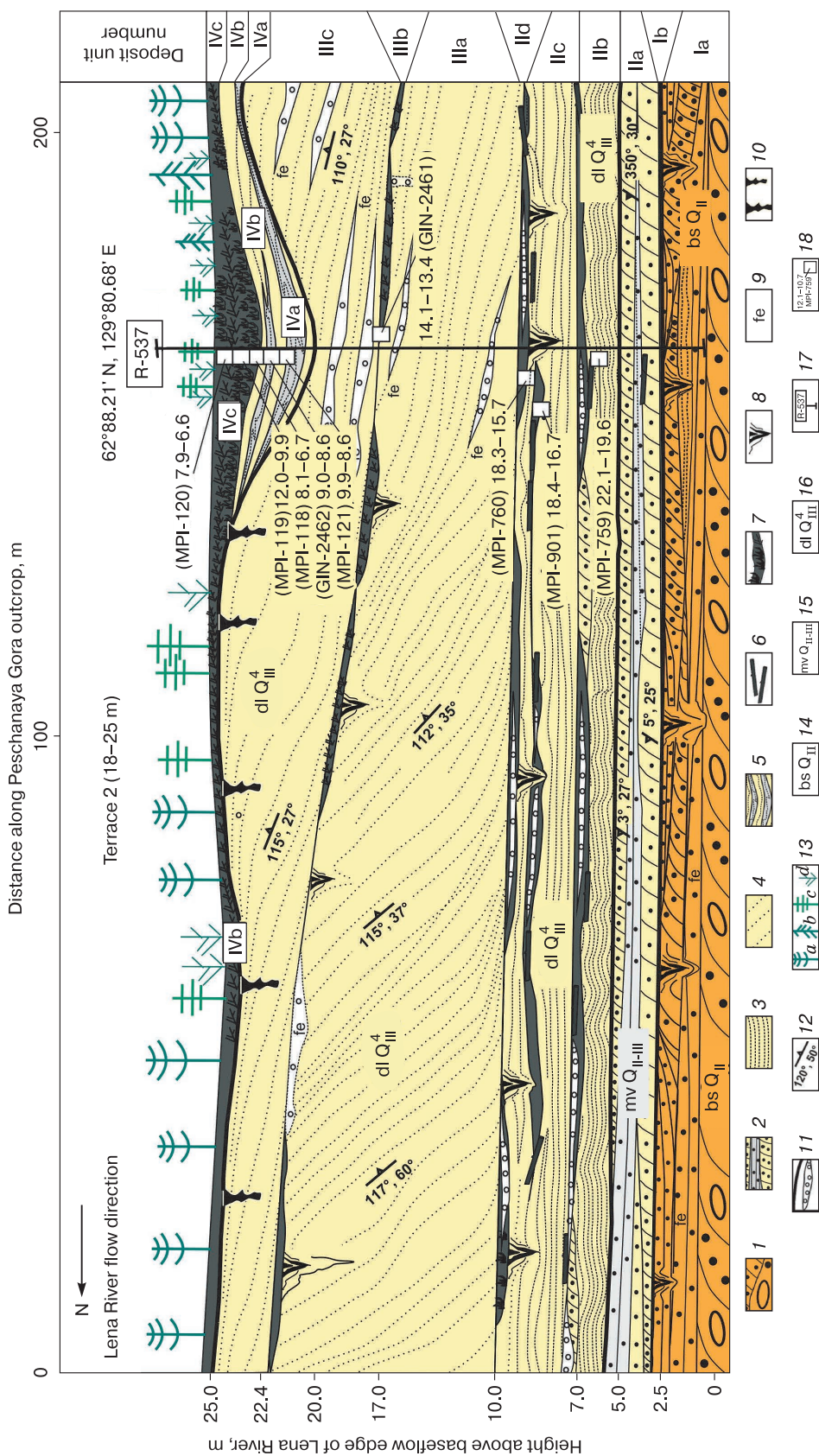


**Fig. 4. Section of 18–25-meter Lena River terrace in the Peschanaya Gora outcrop (Central Yakutia).**

1 – planar stratification of ochre sands with gravel and pebble with planar and oblique lamination; 2 – planar stratification of sands and dusty loamy sand with parallel, lens-like, and oblique lamination; 3 – planar interlayering of ochre sands and loamy sands with translational climbing ripple stratification, adhesion and niveo-aeolian types of lamination, denivation structures, deflationary interlayers of fine gravel; 4 – cross-bedded stratification of light sands with steep inclined grain-fall lamination of the dune slip face, translational climbing ripple lamination, parallel lamination; 5 – interlayering of light sands of grey gleyed loamy sands with intensely deformed lamination and ambiguous lamination; 6 – drift-wood; 7 – peat bogs and paleosol fragments; 8 – sandy wedges and veins; 9 – intense iron hydroxide colouration; 10 – humus nodules and veins; 11 – structural nonconformities and deflation; 12 – strike azimuth and dip angle of layers; 13 – vegetation (a – pine, b – larch, c – birch, d – willow); 14–16 – series designations in accordance with [Kamaleidinov, Minuk, 1997]; 14 – Bestyakh; 15 – Mavrin; 16 – D’oluminskaya; 17 – key clearing in which granulometric and mineralogical sampling was completed; 18 – radiocarbon dates in calibrated k.a. and their laboratory numbers.

everywhere which are densely cemented by epigenetic iron hydroxides and carbonates. The bottom of the unit is not outcropped and is located below the Lena River level. The top of the unit is weakly wavy and outcrops only during periods of severe baseflow.

The granulometric composition of the unit changes abruptly from layer to layer, indicating frequent changes in the energy of the flow, which is typical for aqueous conditions of particle transport and deposition. The mean grain size varies from 55  $\mu\text{m}$  (dusty sand interlayers) to 460  $\mu\text{m}$  (coarse sand layers with a mix of fine gravel). Overall, the average composition of the unit (8 samples) is indicative of moderate sorting and a symmetric normal distribution of particles: the mean grain size ( $x$ ,  $\mu\text{m}$ ) is  $316.8 \pm 64.9$ , the sorting coefficient ( $\sigma$ ) is  $2.03 \pm 0.16$ , skewness ( $\alpha$ ) is  $0.04 \pm 0.10$ , excess kurtosis ( $\tau$ ) is  $1.10 \pm 0.18$ .

The mineralogical composition of the sand fraction (100–50  $\mu\text{m}$ ) of unit Ia (the average of nine samples) is represented by quartz (39.9 %), feldspar (28.1 %), carbonates (20.3 %), amphiboles (7.4 %), and magnetite (1 %).

The unit has planebed stratification composed of interchanging steady, thin (5–10 cm) sandy series with horizontal and oblique lamination typical for aquatic dunes and riffle facies [Botvinkina, 1962; Kutyrev, 1968]. The thickness of the elementary laminae in the oblique series is 1–3 mm, the north strike has a 25–30° dip, and its orientation matches the modern flow of the Lena River. The bottom portions of the elementary laminae are substantially enriched by large and heavy fractions. Series with horizontal lamination are composed of thin (1–5 mm) interchanging layers of light medium-grain sand and grey dusty loamy sand with a mix of fine alluvial organic detritus. Individual layers show small signs of water ripples.

**Unit Ib (2.45–2.50 m)** is a paleosol composed of ochre-coloured loamy sand with thin lenses (3–4 cm) of humified organic detritus and a mix of small charcoal pieces. The mean grain size ( $x$ ,  $\mu\text{m}$ ) is  $56.2 \pm 1.1$ , the sorting coefficient ( $\sigma$ ) is  $4.43 \pm 0.8$ , skewness ( $\alpha$ ) is  $-0.25 \pm 0.15$ , kurtosis is ( $\tau$ )  $0.85 \pm 0.03$ . This indicates very poor sorting and a very platykurtic distribution with tails of fine fractions.

The stratification of unit Ib is gently wavy, the lamination is thin parallel. The top of the unit is sporadically disturbed by secondary vertical sandy veins and small wedges 10–15 cm thick, which extend up to 0.5–1.0 m deep into underlying deposits. The distance between neighboring wedges is 4–6 m. The lateral edges of the wedges are abrupt, deformations are absent in enveloping deposits.

Thus, the features of the structure of units Ia and Ib allow to relate them to a full alluvial cycle, the bottom part of which has channel facies (unit Ia), while the top is marked by floodplain facies (unit Ib) with paleosols and secondary sandy wedges of subaerial genesis.

**Unit IIa (2.5–5.0 m)** is composed of interchanging oblique light sands (5–10 cm) and grey loamy sands (3–10 cm) with thin parallel lamination. The oblique lamination is composed of interchanging elementary laminae from 1 to 10 mm thick, with a strike in the direction of the modern flow of the Lena River (north) and a 25–30° dip. The elementary laminae clearly differ from one another in color and granulometric and mineralogical composition. Dark laminae are enriched by heavy minerals, light laminae show a higher content of mica and quartz. The unit top shows evidence of ripple marks, alluvial organic detritus lenses, small charcoal pieces, thin interlayers of fine gravel (1–3 mm).

**Unit IIb (5.0–7.0 m)** is composed of well-sorted light sands with thin (0.5–2.0 mm) systematic horizontal and wavy colmatage interlayers of dark loamy sands which repeat every 2–5 cm. The step between adjacent interlayers is maintained at a long horizontal distance (3–5 m or more), the bends of each interlayer repeat the previous one. The top portion of the unit shows interlayers (1–3 cm) of large-grain, loose, gravelly quartz sand with a mix of humified organic detritus and small charcoal pieces (Fig. 5, b).

The granulometric composition (two samples) of unit IIb deposits indicates moderate sorting and a flat symmetric distribution: the mean grain size ( $x$ ,  $\mu\text{m}$ ) is  $253.9 \pm 10.9$ , the sorting coefficient ( $\sigma$ ) is  $1.84 \pm 0.16$ , skewness ( $\alpha$ ) is  $-0.06 \pm 0.02$ , kurtosis ( $\tau$ ) is  $0.82 \pm 0.06$ . Coarsening of the granulometric composition is seen inside the layers, upward from the bottom to the top (inverse grading).

Parallel wavy adhesion lamination is typical for unit IIb (Fig. 5, e). The distance between the interlayers is not continuous and changes from several millimeters to 3–4 cm. Each of the interlayers is ferruginated to a different extent. In some parts the thickness of the interlayers increases to 2–4 mm. Such structure types are called adhesive climbing ripple lamination, which forms from aeolian deposition of sand grains onto a humid sedimentation surface [Huissteden et al., 2000; Brookfield, 2011; Caputo, 2020]. Some colmatage interlayers are made more complex by vertical micro-wedge-like apophyses up to 1–2 cm in size, the origin of which most researchers relate to the melting of niveo-aeolian deposits and infiltration by surface waters [Huissteden et al., 2000].

**Unit IIc (7.0–9.85 m)** differs from the underlying unit in only one sedimentational structure type. Here, colmatage interlayers become rather thin, straight, and difficult to tell apart. The distance between neighboring interlayers becomes more steady, and the structure itself more uniform (Fig. 5, b). Unlike the underlying unit IIb, the colmatage interlayers are composed not of silty material, but of fine magnetite grains. This type of structure forms under the condition of sand particle deposition onto a dry surface and is called translent climbing ripple lami-

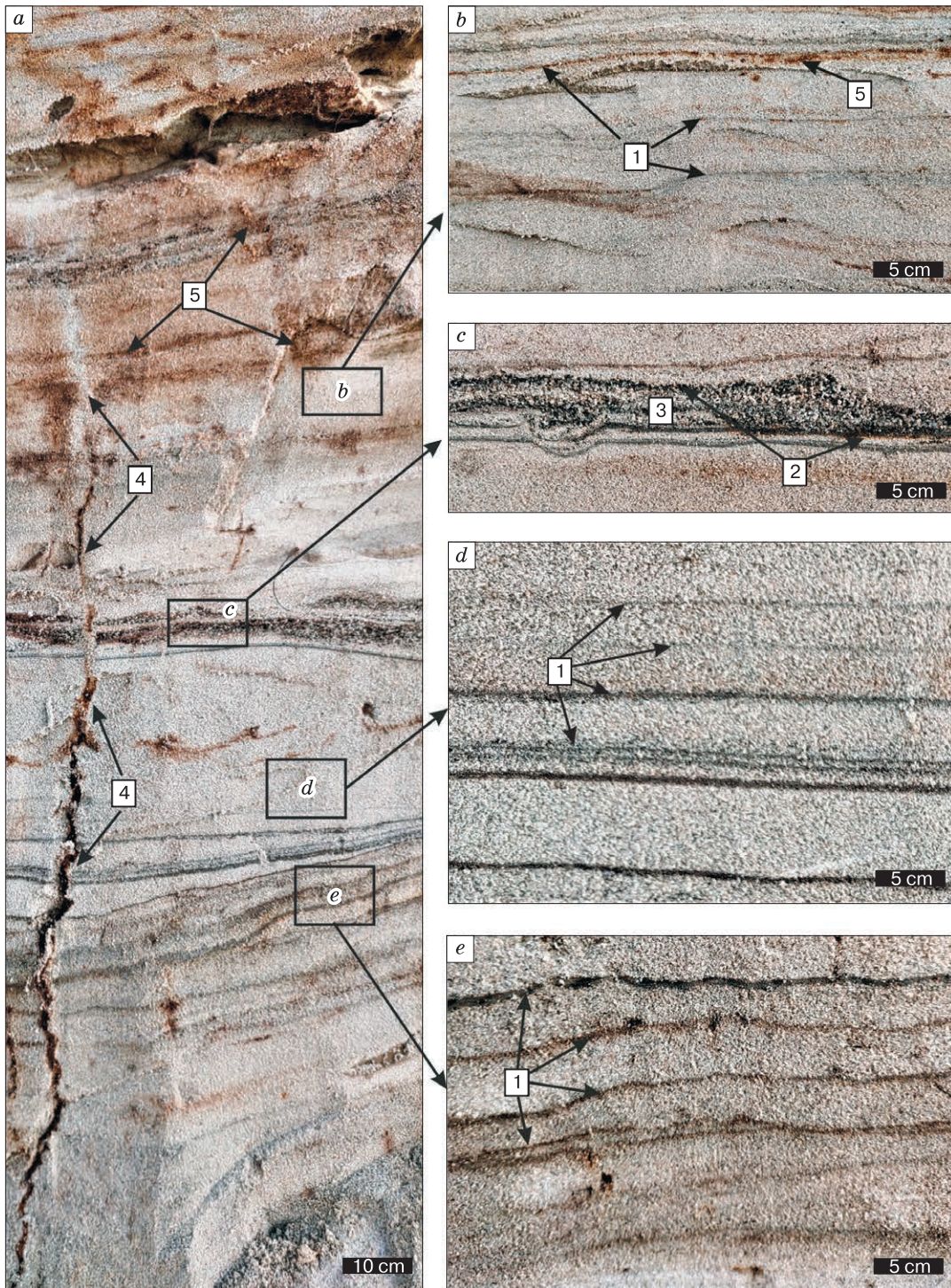


**Fig. 5. Some types of adhesion lamination of the D'olkuminskaya Series in the Peschnaya Gora outcrop.**

Units IIb, IIc (6.0–8.0 m): *a* – overall appearance; *b* – wavy adhesion climbing ripple lamination; *c* – deflation horizon with paleosol; *d* – parallel planebed adhesion lamination; *e* – wavy-crinkly stratification and adhesion lamination. 1 – elementary sedimentation surfaces; 2 – humified sand (paleosol); 3 – large sand with fine gravel; 4 – epigenetic fracture of vertical groundwater infiltration; 5 – post-sedimentational ochre striation. A.A. Galanin's photo from September, 2020.

nation [Hunter, 1977; Huissteden et al., 2000; Boggs, 2009; Brookfield, 2011].

**Unit II d (9.85–10.0 m)** is a paleosol which is composed of thin interlayering of large-grain sand and dark humified loamy sand with fine vegetative detritus, alluvial organic matter lenses, and is divided in places by secondary vertical sandy veins and wedges up to 1.5 m deep and up to 0.5 m wide, filled with quartz sand from overlying layers.

The mineralogical composition of the sand fraction (100–50  $\mu\text{m}$ ) of units II b and II c (the average of eight samples) is represented by quartz (44.2 %), feldspars (36.8 %), carbonates (9.7 %), amphiboles (5.3 %), epidote (1.4 %), and magnetite (1.1 %).

In general, intense diagenetic striation formed by lines, crinkly films and ochre stains (Fig. 5) is typical for units II b and II c. Sometimes the striation inherits the sedimentational stratification, but intersects it in most cases. The complex geometry of the striation is clearly related to the uneven upward movement of the bottom of the active layer during syngenetic freezing of the deposits. Numerous intensely ferruginated vertical fractures up to 2–3 cm thick and up to 1.5–2.0 m long (Fig. 5, a) are also seen in unit II.

**Unit III a (10.0–17.0 m)** is composed of well-sorted light sands with infrequent interlayers of large-grain quartz sand and thin lenses of fine gravel (2–4 mm). The mean granulometric composition of the unit (two samples) is indicative of moderate sorting and a leptokurtic symmetric distribution: the mean grain size ( $x$ ,  $\mu\text{m}$ ) is  $298.4 \pm 79.5$ , the sorting coefficient ( $\sigma$ ) is  $1.70 \pm 0.04$ , skewness ( $\alpha$ ) is  $0.02 \pm 0.01$ , excess kurtosis ( $\tau$ ) is  $1.12 \pm 0.36$ . The bottom and top of the unit are abrupt, cut off by the deflation surfaces (Fig. 3, Fig. 6, a). The mineralogical composition of the sand fraction (100–50  $\mu\text{m}$ ) of unit III a (the average of four samples) is represented by quartz (47.4 %), feldspars (35.1 %), carbonates (4.0 %), amphiboles (5.1 %), magnetite (3.1 %), and small charcoal pieces (3.0 %).

The unit is composed of inclined (diagonal) series up to 2–3 m thick with clearly defined grain-fall cross-stratification of the dune slip-facies [Hunter, 1977]. The stratification has a southeast strike (112–115° azimuth) with a 35–45° dip, which matches the orientation of the dunes on the surface of the adjoining terrace and is opposite to the modern flow of the Lena River.

The texture is represented by grain-fall lamination [Hunter, 1977; Brookfield, 2011]. It is caused by granulometric and mineralogical heterogeneity, as well as the varying density of grain packing in elementary laminae, the thickness of which is 2–4 mm. Some laminae are enriched by humus, fine vegetative detritus, and present as poorly developed paleosols, which are indicative of a short-lived dune slip face fixing by a vegetative cover (Fig. 6, a–c). The epigen-

etic stratification and staining formed by colmatage interlayers and iron hydroxide stains are also indicative of this.

**Unit III b (17.0–17.4 m)** is a deflational surface underlain by dark sand and loamy sand with paleosol fragments. The surface discordantly cuts off the inclined series of the underlying unit (III a), has a southeast strike at 10–15°, and is disturbed by vertical sand veins up to 10–15 cm thick and up to 0.5–1.0 m deep. The paleosol is formed by discontinuous thin (0.5–1.0 cm) interlayers and lenses of fine vegetative detritus, small charcoal pieces, thin interlayers of bleached large-grain quartz sand with a mix of fine (2–3 mm) gravel, and abnormally high concentrations of magnetite and zircon in the fine fraction.

The granulometric composition (two samples) indicates moderate sorting. The mean grain size ( $x$ ) varies from 980 to 317  $\mu\text{m}$ , the sorting coefficient ( $\sigma$ ) is  $1.71 \pm 0.23$ , skewness ( $\alpha$ ) is  $-0.39 \pm 0.10$ , excess kurtosis ( $\tau$ ) is  $1.23 \pm 0.06$ . Clearly defined negative skewness, a leptokurtic distribution, and enrichment by the coarse fraction indicate a significant deflation lag.

**Unit III c (17.4–20.0 m)** is composed of well-sorted medium-grain sands with interlayers of large-grain bleached sand and rare inclusions of thin soil-peat interlayers up to 2–4 cm thick. The granulometric composition of the unit (eight samples) indicates moderate sorting, a flat asymmetric distribution with “tails” of fine fractions: the mean grain size ( $x$ ,  $\mu\text{m}$ ) is  $240.2 \pm 17.0$ , the sorting coefficient ( $\sigma$ ) is  $1.69 \pm 0.06$ , skewness ( $\alpha$ ) is  $-0.16 \pm 0.07$ , kurtosis ( $\tau$ ) is  $0.81 \pm 0.07$ . This indicates blowing out of the dusty fraction and enrichment by coarse particles.

The mineralogical composition (the average of six samples) of the sand fraction (100–50  $\mu\text{m}$ ) is represented by quartz (50.7 %), feldspars (38.8 %), amphiboles (5.6 %), magnetite (1.7 %), and carbonates (0.9 %).

The structure of unit III c is formed by several cross-bedded series divided by deflational surfaces and representing mostly steep leeward dune slope slipfaces and gentle windward slope faces consisting of climbing ripples. Translational climbing ripple stratification with a southeast strike (110° azimuth) with a 15–25° dip dominates in most series. This strike matches the dune orientation at the surface adjoining the terrace outcrop and is opposite to the modern flow of the Lena River.

Some gently inclined series up to 30–40 cm thick demonstrate thin parallel lamination (Fig. 6, e), others show translational climbing ripple lamination (Fig. 6, e–g). A signature feature of the deposits is the presence of bright epigenetic ochre striation.

The top of unit III c outcrops onto the modern surface as vegetated U-shaped and longitudinal dunes of southeast orientation. These dunes cover the entire surface of the Kerdyom terrace on the right bank of

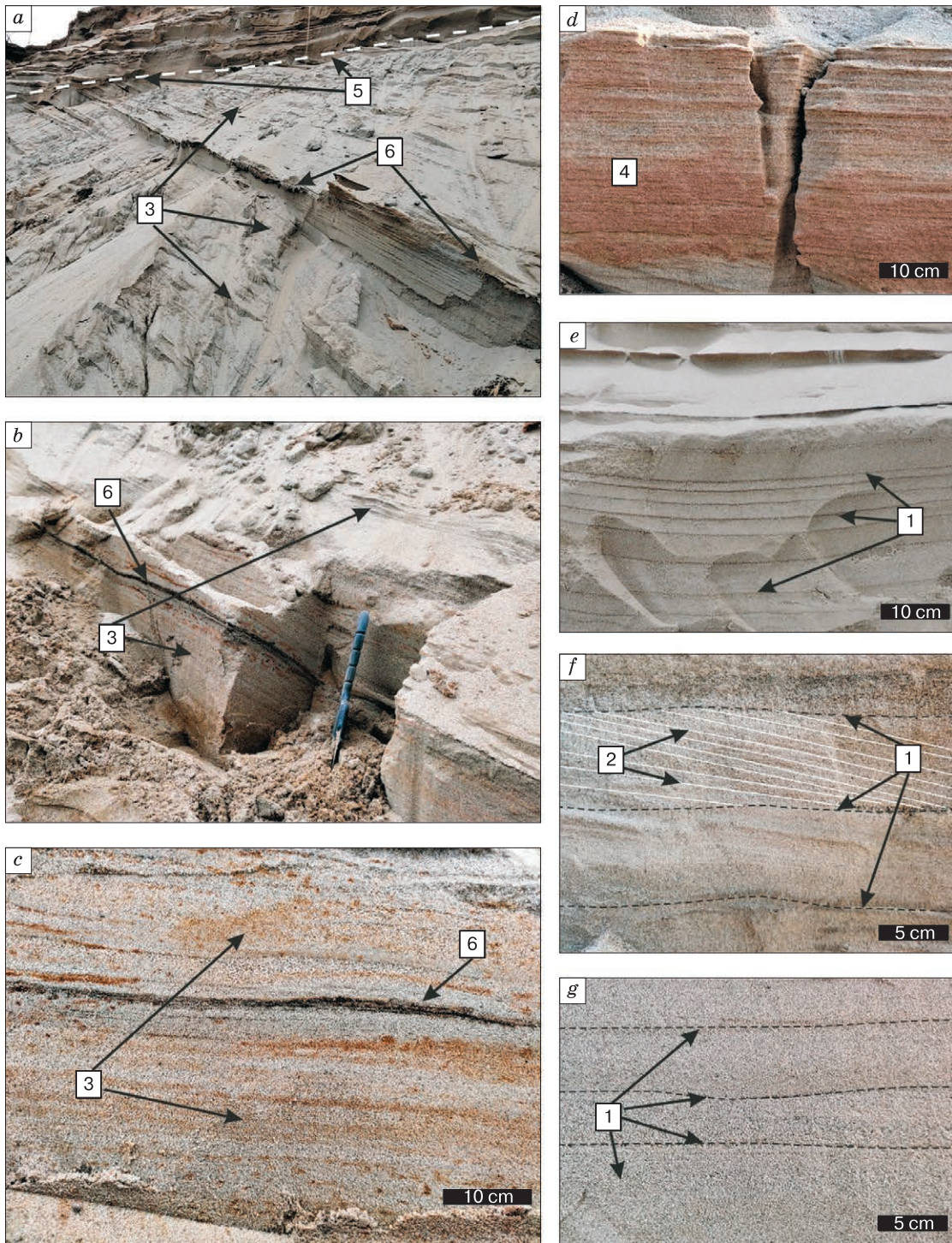


**Fig. 6. Some types of D'olkuminskaya Series stratification and lamination in the Peschanaya Gora outcrop.**

Units IIIa, IIIb (10.0–20.0 m): *a, b* – cross-bedded stratification of the dune slip face facies (unit IIIa); *c* – grain-fall dune slip face lamination facies (unit IIIa); *d* – planar parallel lamination (unit IIIb); *e–g* – translantent climbing ripple stratification (unit IIIb). 1 – translantent interlayers composed of magnetite grains; 2 – climbing ripple lamination; 3 – grain-fall dune slip face lamination; 4 – parallel planar lamination; 5 – structural nonconformity (deflation); 6 – paleosol marking a short-term period of dune slip face fixing by vegetation. A.A. Galanin's photo from September, 2020.

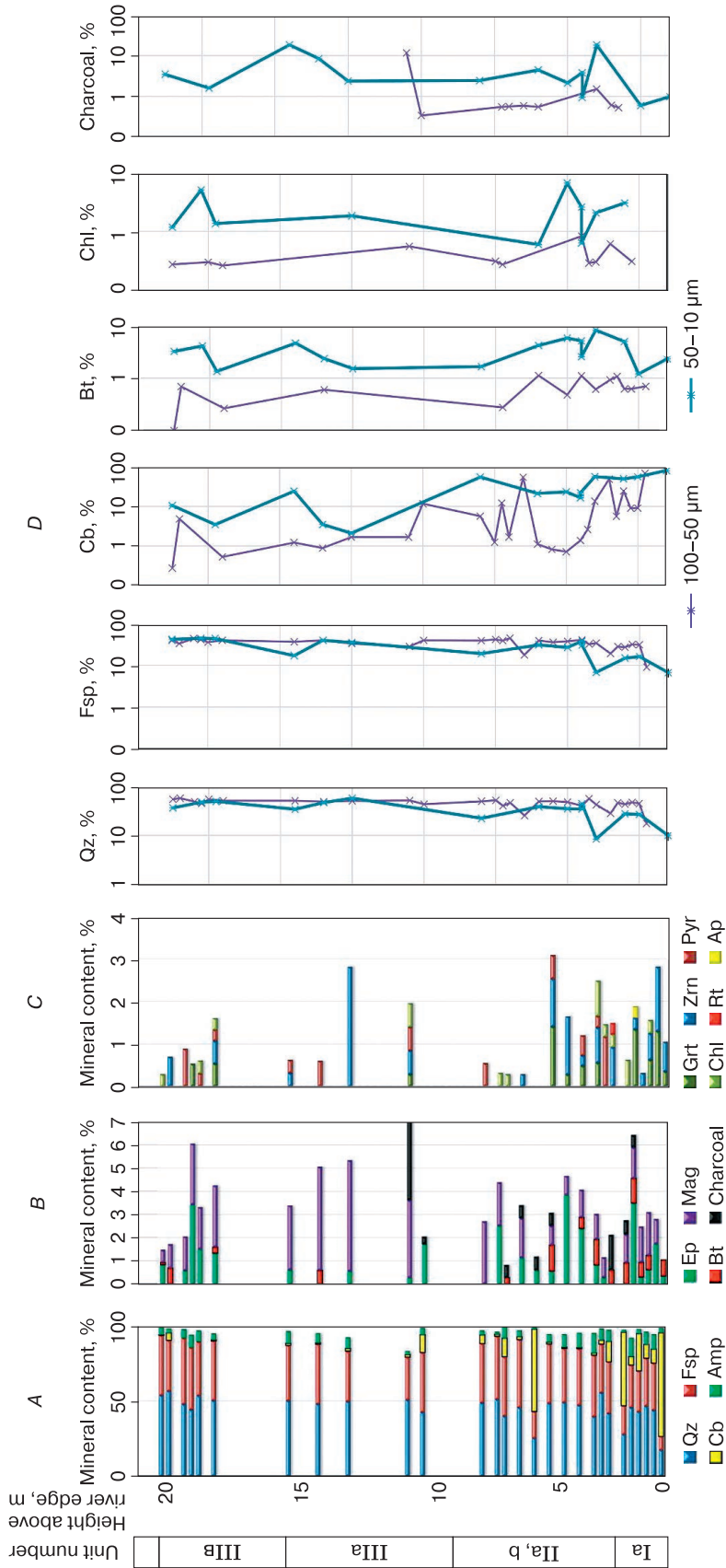


**Fig. 7. Mineralogical composition of Peschanaya Gora key section deposits by the R-537 clearing (middle course of the Lena River, Eastern Siberia).**

A-C – mineral content of 100–50 μm fraction (A – primary, B – secondary, C – accessory); D – mineral content of 100–50 μm and 50–10 μm fractions; Qz – quartz, Fsp – feldspar, Cb – carbonate, Amp – amphibole, Ep – epidote, Bt – biotite, Mag – magnetite, Grt – garnet, Zrn – zircon, Pyr – pyroxene, Chl – chlorite, Rt – rutile, Ap – apatite; charcoal.

the Lena River, from the Suola River mouth to the Aldan River mouth. The dune brinks are divided by gently sloping interdune depressions, which are currently occupied by lakes and swamps. One such paleobasin is exposed by natural erosion in the southern part of the Peschanaya Gora outcrop at the R-537 section (Fig. 4).

**Unit IVa (20.0–20.4 m)** is composed of interchanging layers (5–10 cm) of well-sorted light sand and interlayers (4–5 cm) of dense bluish-grey gleyed light loam without visible organic matter. The granulometric composition (one sample) of the loam indicates very poor sorting and positive skewness with a modal value bias toward fine fractions: the mean grain size ( $x$ ,  $\mu\text{m}$ ) is 44.5, the sorting coefficient ( $\sigma$ ) is 4.29, skewness ( $\alpha$ ) is 0.13, excess kurtosis ( $\tau$ ) is 0.95. The stratification of the deposits is gently wavy, sometimes deformed into microfolds with signs of boudinage.

Apparently, the reason for poor sorting of the deposits is the interchanging lake and aeolian sedimentation regimes under conditions of a small seasonal body of water surrounded by unvegetated dunes.

**Unit IVb (20.4–22.4 m)** is composed of interchanging light well-sorted sands with thin interlayers of dark grey fine sands and dusty loamy sands. There are no visible organic remains. The granulometric composition (five samples) is as follows: the mean grain size ( $x$ ,  $\mu\text{m}$ ) is  $316.9 \pm 30.7$ , the sorting coefficient ( $\sigma$ ) is  $1.67 \pm 0.16$ , skewness ( $\alpha$ ) is  $-0.21 \pm 0.07$ , excess kurtosis ( $\tau$ ) is  $1.18 \pm 0.15$ . This indicates moderate sorting and enrichment by large fractions. The stratification is subhorizontal, intensely deformed here and there in the form of traction microfolds, microdiapirs, vertical fractures with a 10–15 cm displacement. Lamination is unclear.

Unlike the underlying unit (IVa), there is coarsening of the granulometric composition from the bottom to the top of the unit (inverse grading). Intense layered coloring of deposits by iron hydroxide is also typical. The top of the unit is abrupt, clear, composed of well-sorted bleached sand.

**Unit IVc (22.4–25.0 m)** is a dense, dark brown peat bog with numerous large fragments of moss and subshrub vegetation, wood fragments. It delaminates well into horizontal plates, has interlayers of bleached coarse sand in the bottom portion. Sedge peat with a mix of quartz sand and numerous small (1–4 mm) mollusk shells dominates the bottom portion. The top portion is a moss-subshrub peat with a mix of wood fragments. Apparently, the peat bog formed by way of a small lake overgrowing.

#### Mineralogical composition of aeolian sand covers

The mineralogical composition and features of mineral distribution in the section are important facies attributes of aeolian deposits in the cryolithozone [Pewe, *Journaux*, 1983; Dijkmans *et al.*, 1986, 1988].

The main minerals in both studied fractions (100–50 and 50–10  $\mu\text{m}$ ) of the deposits of the Peschanaya Gora outcrop 25-meter Kerdyom terrace are quartz, feldspars, calcium carbonates, amphiboles, and magnetite (Table 2, Fig. 7).

In the 100–50  $\mu\text{m}$  fraction the total composition of the main minerals exceeds 95 %. The mean quartz content increases up the section approximately by 10 % from 39.9 % in unit Ia to 50.7 % in unit IIIc. The mean feldspar content also increases from 28.1 % to 38.8 %. Carbonate mineral distribution is quite uneven. Their maximum content (20.3 %) is concentrated in the secondary thin iron-carbonate crusts (calcretes) of unit Ia, and in some individual samples of this unit the carbonate mineral content reaches 68 %. The minimum contents (0.9 %) are found in unit IIIb. Amphibole content decreases insignificantly up the section from 7.4 % in unit Ia to 5.4 % in unit IIIc.

Magnetite, biotite, and epidote are always present among secondary and accessory mineral groups in the 100–50  $\mu\text{m}$  fraction. Most samples also have zircon, garnet, chlorite, grains of hard coal. Some samples show individual grains of pyroxenes, apatite, rutile, ochre-colored iron hydroxides. A characteristic feature is a significant (threefold) increase in heavy fraction and magnetite content up the section. Thus, the gravel-pebble-sand deposits of unit Ia have a mean magnetite content of approximately 1 %, and it reaches 3.1 and 1.7 % in units IIIa and IIIc, respectively, while in some samples from the top of unit IIIa the magnetite concentration reaches 4.8 %. At the same time, some of the higher concentrations of zircon (2.8 %) and micro particles of charcoals (11.7 %) are seen here.

From the bottom to the top of section the variation of primary and secondary minerals is even more contrasting in the 50–10  $\mu\text{m}$  fraction, but, overall, repeats their distribution in the 100–50  $\mu\text{m}$  fraction. Thus, the mean quartz content increases from 18.8 % in unit Ia to 41.4 % in unit IIIc. Feldspar content increases from 11.1 % in unit Ia to 43.0 % in unit IIIc. Carbonate content decreases from 46.6 % in unit Ia to 5.3 % in unit IIIc. Variations of accessory minerals in this fraction are significantly smaller, but are 2–3 times higher overall in comparison to the 100–50  $\mu\text{m}$  fraction. The concentration of readily solvable carbonates in some samples of unit Ia reaches 70–80 %. The carbonates are represented both by whole grains and by fine crystalline aggregates coating the grains of other minerals as a crust. The minerals dissolve completely in a 5 % HCl solution.

#### The lithological source of aeolian sand cover formation

Based on primary mineral proportions, all studied samples of D'olkuminskaya Series sand covers from the Peschanaya Gora outcrop are oligomictic

arkose-quartz sands. The same series' sands, studied by the author earlier [Galanin *et al.*, 2018] in the basin of the lower course of the Vilyuy River, differ significantly in their mineralogical composition. The series is composed of monomictic quartz sands with an 80–95 % quartz content and small amounts of feldspars (<9 %) on the Kysyl-Syr portion of the outcrop. Furthermore, significant concentrations of magnetites, zircons, and secondary carbonates have not been identified here. At the same time, accessory mineral content is significantly higher, and their composition is more diverse (garnet, epidote, hornblende, pyroxene, ilmenite, leucoxene, agate, chalcedony, etc.). Such significant differences can be explained by different origins of feeding sources of Quaternary alluvium in the basins of the Vilyuy and Lena rivers.

Indeed, the identified differences in the mineralogical composition of the D'olkuminskaya Series in the Peschanaya Gora (middle course of the Lena River) and Kysyl-Syr (lower course of the Vilyuy River) outcrops agree with the mineralogical zoning map of the Vilyuy syncline of A.G. Kossovskaya [1962]. The Peschanaya Gora outcrop is linked to the Yakut-Sinskiy garnet-zircon sub-province, the formation of which is related to the denudation of the crystalline base rocks within the Aldan and Stanovoy highlands. A direct feeding source of Quaternary deposits (including alluvium) here is the Jurassic greywacke-quartz sandstones with a quartz content of 50–66 %. Their characteristic feature is the presence of zircon and high concentrations of magnetite, which explains the constant presence of these minerals in the deposits of Peschanaya Gora.

The Kysyl-Syr outcrop is linked to the Vilyuy-Tyungsk epidote-ilmenite-amphibole mineralogical province, the feeding areas of which are the Archean-Proterozoic crystalline rocks of the Patomsk Highland [Kossovskaya, 1962]. A direct source of Quaternary alluvium and D'olkuminskaya Series sands in the basin of the lower course of the Vilyuy River is the Late Cretaceous quartz-oligomictic sandstones which compose long areas of river cliffs. They are weakly cemented and break easily, forming vast quartz-kaolinite weathering rinds on gently sloping drainage divides. Cretaceous sandstones are enriched by quartz (65–80 %) and are extremely lacking in heavy minerals. This explains the high quartz content (80–95 %) and rather low magnetite content in the D'olkuminskaya Series deposits of the Kysyl-Syr outcrop. Among secondary minerals epidote, amphiboles, kaolinite, opal are always present in this mineralogical province [Kossovskaya, 1962].

#### **Sand and loess-ice (Yedoma) covers – two lithological derivatives of Quaternary alluvium**

T.L. Pewe and A. Journaux's work [Pewe, Journaux, 1983] is dedicated to the study of the mineralogical composition of cover loess-ice and sand deposits

of the high terraces of the Lena River. The authors studied the mineralogical composition of 28 samples collected within the Lena-Amga interfluvium. It was established that the primary components of both sand and loess-ice covers in Central Yakutia are quartz, mica, and feldspars, which, together, total 80–90 %. There are calcium carbonates, the content of which reaches 7.6 % in all the samples, with the exception of modern alluvium. Amphiboles and epidote dominate in the heavy fraction, small amounts of pyroxenes, titanite, garnet, zircon are present, rutile, tourmaline, kyanite, monazite, anatase, and others are occasionally seen. Overall, researchers conclude that the loess-ice (Yedoma) and sand covers (D'olkuminskaya Series) of the Lena-Amga interfluvium belong to aeolian deposits and are two granulometric derivatives – the products of wind reworking of the Lena River's Quaternary alluvium [Pewe, Journaux, 1983].

A clear signature of aeolian genesis of the cover sands is the high concentration of magnetite and other heavy minerals, as well as secondary, readily soluble carbonates. The latter can be found in the form of carbonate-ferruginous films (carbonate mycelium) and are called calcretes [Dijkmans *et al.*, 1986, 1988]. Constant presence of calcretes and iron hydroxides is typical for the Late Quaternary aeolian sands of the Kobuk dune massif in the Alaskan northwest and is an important genetic attribute which indicates hyperarid deposition conditions [Dijkmans *et al.*, 1986, 1988].

The aforementioned mineralogical attributes are typical for units IIb, IIc, IIIa, IIIc of the Peschanaya Gora outcrop (Table 2). In comparison to the underlying alluvium (unit Ia) they show a threefold increase in magnetite content. The deflational lag (unit IIIb), which divides the lower (unit IIIa) and upper (unit IIIc) parts of the D'olkuminskaya Series sands, is most enriched by zircon (2.8 %), magnetite (4.8 %), and small pieces of charcoal (11.7 %) at the 17.0–17.4 m interval from the water edge of the Lena River. A high concentration of the heavy fraction at the unit borders may be related to a significant deflation lag and accumulation of wind eluvium.

A constant presence of trivalent iron hydroxides (limonite, ochre) which create an epigenetic striation of a bright ochre color, which indicates good aeration and alkaline sedimentation conditions, is typical for D'olkuminskaya Series deposits. The light and, in some spots, ochre color of the deposits, the lack of reduction minerals (vivianite) are additional criteria for subaerial origin of the deposits.

#### **Stratification and lamination of aeolian sand cover**

The structure of aeolian sand cover forms under the influence of numerous factors: wind speed, presence and volume of source loamy sandy material, strike and extent of humidification of the surface at

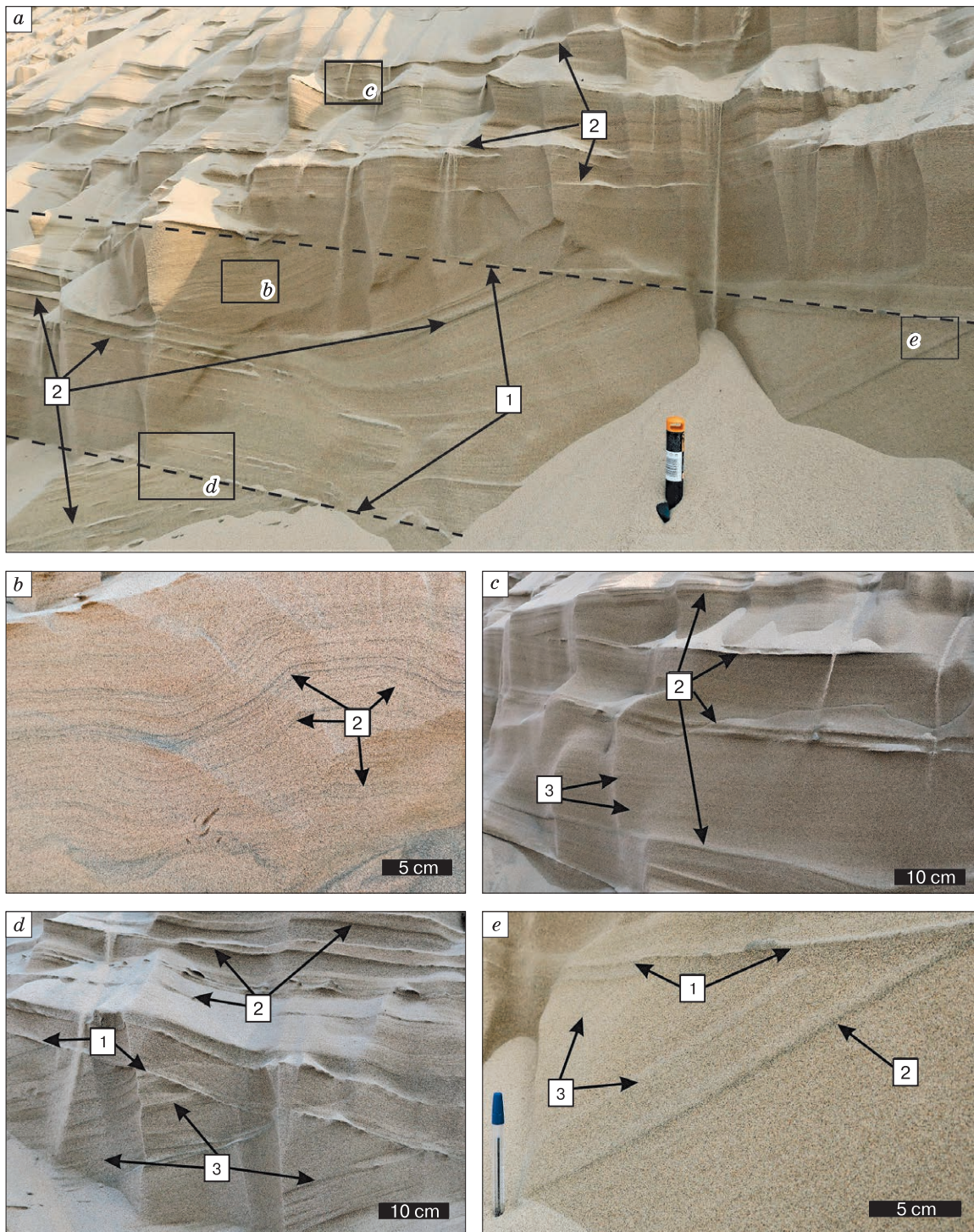


**Fig. 8. Cross-bedded structure and translant climbing ripple lamination in D'olkuminskaya Series dune deposits (Ust'-Buotama outcrop of the 75–100-meter terrace (Bestyakh) of the Lena River, lower portion).** *a* – overall appearance of the unit with a clear cross-bedded structure and translant climbing ripple lamination; *b–e* – enlarged fragments of individual series with different geometric characteristics (dip angles) of stratification and lamination. 1 – abrupt deflation borders between sandy series; 2 – translant interlayers (pseudo-stratification) composed of magnetite grains; 3 – elementary translant climbing ripple lamination laminae. A.A. Galanin's photo from August, 2020.

the moment of sedimentation, temperature of the deposits, presence of snow cover, vegetation type. According to R.E. Hunter [1977] and his followers, the structure of aeolian sand cover differs drastically from other genetic types of deposits, including alluvium. The structure of aeolian sand cover is characterized by several key types of stratification and lamination.

*Planebed stratification* and *planebed lamination* [Hunter, 1977; Brookfield, 2011] form simultaneously in areas of more intense wind load. Such conditions are not favorable for aeolian ripple formation, and accumulation is very slow. The deposits have a coarsened composition and are characterized by dense packing of sand grains (minimal porosity). These stratification and lamination types are more typical for aeolian sand covers of small thickness, gently sloping windward dune slopes, and deflation basins. In the D'olkuminskaya Series deposits planed parallel lamination series are usually found on the borders of large cross-bedded units, as well as near the top.

*Cross-bedded stratification* [Hunter, 1977; Brookfield, 2011] is represented by large units from 1 to 6–10 m thick, separated from one another by structural nonconformities – deflation surfaces (Fig. 6, *a* and Fig. 8, *a*), also called *deflation lags* by Western authors [Waters et al., 1999; Brookfield, 2011; Derbyshire, Owen, 2017]. Each elementary unit is different in the nature and incline orientation of the bottom and top, the thickness of the elementary laminae, the amplitude and nature of the inclination. Essentially, each unit is a particular fragment of the fossil dune. Each unit forms owing to continuous movement of dunes across the dune field, as a result of which each consecutive dune creeps over and/or partially cuts off the previous ones. The individual segments of the deflation surfaces are often enriched by wind eluvium – large and heavy fractions sometimes containing fine gravel, ventifacts, vegetation detritus, small charcoal pieces, bones of small animals, remains of thin soil-divot horizons. Deflation surfaces are usually flat, sometimes gently sloping, nonconformingly cut off the inner stratification of elementary units in their top and bottom.

*Cross-bedded mesostratification* (Fig. 6, *b*) has a principally different originating mechanism. In aeolian deposits it is typical for the slip face facies and is called *grain-fall cross-stratification* or *dune-slipfacies cross-bedding* [Hunter, 1977; Kasse, Aalbersberg, 2019]. The formation of this facies occurs as a result of systematic falling (rolling down) of sand grains from the dune brink and their deposition on the leeward dune-slope or slip face. Fixing of falling grains on the steep leeward slope occurs by way of rather weak cohesion with the bedding surface, which leads to the formation of a thin and loose, barely noticeable *grain-fall lamination* [Hunter, 1977; Brookfield, 2011]. In the longitudinal section of a parabolic dune the

elementary laminae dip at 35–45° in the direction of its movement.

*Sandflow lamination* is also common within the dune slip face facies [Hunter, 1977; Brookfield, 2011]. It forms as a result of periodic gravitational slumping of small portions of sand down from the slip face brink, as a result of which fan-shaped cones form at the foot of the lee-slope. Aeolian dune deposits with cross-bedded stratification, including the Peschanaya Gora outcrop, are often incorrectly interpreted by some researchers as oblique alluvial stratification [Bolshiyakov et al., 2016; Pravkin et al., 2018]. Aside from numerous other differences, aeolian dune cross-bedded stratification has a larger size, comparable with the size of elementary parabolic dunes, the height of which varies from 4 to 8 m in Central Yakutia.

*Wavy bedding* is widely presented in D'olkuminskaya Series deposits, and forms by way of burial of aeolian ripple marks that migrate across the surface on the border of aeolian units. The length of the ripples usually varies from 20–30 cm to 1–2 m, the height from 2–3 cm to 5–15 cm. An indicator of aeolian genesis of the ripple marks is their distribution not only on gently sloping, but also on steep areas of the dunes, while water-formed ripples are linked only to horizontal areas and are limited to the height of the water surface. Furthermore, the relationship between the length of the ripple and its height in water-formed ripple marks (equal to 15) is always higher than in aeolian ripple marks (9) [Brookfield, 2011]. The texture of dune deposits with wavy bedding more often manifests as *ripple foreset cross-lamination* and *ripple-form lamination* [Hunter, 1977].

*Translatent climbing ripple stratification* is a specific genetic structural group which is typical only for aeolian deposit dune facies [Hunter, 1977; Brookfield, 2011]. This structure, also known as pseudo-stratification, forms in the process of rather intense aeolian accumulation on gently inclined, predominantly windward dune slopes and horizontal surfaces covered with aeolian ripple marks (Fig. 9).

Aeolian ripple migration across a bedding surface occurs by way of a wind current flow dragging thin parallel laminae on slip face microslopes. This leads to the formation of *climbing ripple lamination*, the elementary laminae of which are parallel to each other and whose strike coincides with the direction of aeolian transfer. The thickness of the laminae usually does not exceed 0.5–3.0 mm, the dip varies from 2–3° to 10–15°. This type of lamination is usually almost unidentifiable on humid outcrop walls and manifests after they dry naturally (Fig. 8, *c–e*).

With a sufficient influx of sandy material and moderate wind loads, the bedding surface continuously moves upward as the ripples move, which leads to the formation of thin translantent interlayers or pseudo-stratification [Hunter, 1977]. Its key differ-

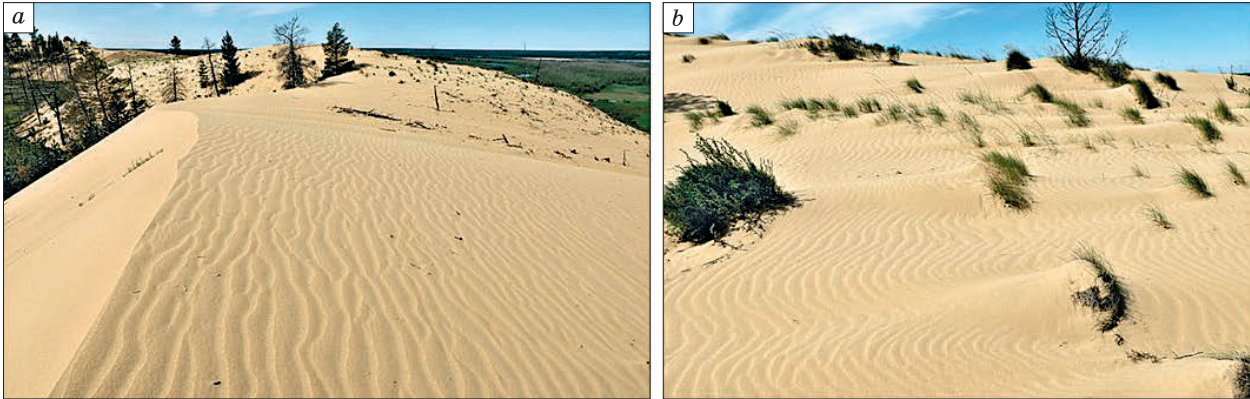


**Fig. 9. Climbing aeolian ripple on some elements of the modern dune relief in the basin of the lower course of the Vilyuy River (Central Yakutia).**

*a* – inclined windward slope near the brink of the parabolic dune; *b* – on the subhorizontal surface, partially fixed by cereal tussocks. A.A. Galanin's photo from July, 2019.

ence from regular stratification is that translant interlayers are not sedimentation surfaces, but are pointed toward it at an angle.

The formation of all translant interlayers in the elementary sand series takes place simultaneously and is linked to the accumulation of heavy minerals in the crests of aeolian ripples. Because of this, the translant interlayers are usually composed of magnetite and stand out sharply against the light quartz sand in which they are contained (Fig. 8, *e*).

Translant interlayers are clearly visible in sections, while the lamination of the ripples themselves, which are composed of mineralogically and granulometrically homogenous elementary laminae, is hard to identify. It is necessary to keep in mind that the azimuths and dips of translant interlayers and lamination are opposite one another. The former is oriented against the wind, and the latter in the direction of the wind.

The identification of translant climbing ripple lamination and the assessment of its geometry play a defining role in the analysis of facies composition and deposit genesis, the reconstruction of the direction of aeolian transport of material. Contrasting and noticeable translant interlayers (pseudo-stratification), represented widely in some D'olkuminskaya Series sand units, have been interpreted by many predecessors as regular alluvial stratification [Map..., 1959; Map..., 1983; Ershov, 1989; Bolshiyarov et al., 2016; Spektor et al., 2016, 2017; Pomortsev et al., 2017; Pravkin et al., 2018], which has led to an incorrect understanding of the overall structure of the deposits and their facies affiliation alike. The taxonomy and formation mechanisms of translant climbing ripple stratification and lamination are reviewed in detail in many works [Hunter, 1977; Brookfield, 2011; Fenton et al., 2013].

*Adhesion stratification and lamination* form as a result of adhesion of aeolian particles to humid surfaces [Kasse, 2002; Zieliński et al., 2015; Kasse, Aalbersberg, 2019]. Their characteristic feature is contrasting and clearly visible, systematic, thin, crinkly interlayers of dark dust which deposit on dune surfaces while they are humid and there is no deflation. Wide distribution of adhesion structures in sand deposits indicates significant fluctuations in humidification during deposition. The nature of humidification of the sedimentation surface is affected by the frequency and amount of atmospheric precipitation, exposure, depth of permafrost aquitard position, river flood level, etc.

For convenience of facies analysis of aeolian deposits C. Kasse and G. Aalbersberg [Kasse, 2002; Kasse, Aalbersberg, 2019] suggested dividing all types of sedimentational aeolian structures into two genetic groups. The first includes structures which form during aeolian sedimentation of particles onto a dry sedimentation surface (dry aeolian lamination). Such structures include grain-fall lamination of dune slip face slopes, some types of translant climbing ripple lamination, etc. [Kasse, Aalbersberg, 2019]. The second group of structures is related to the sedimentation of aeolian particles onto humid and wet surfaces (wet aeolian lamination). It includes different types of adhesion lamination, including *planebed*, *crinkly ripple*, etc. [Kasse, Aalbersberg, 2019].

Seasonal humidification dynamics lead to pulsation of aeolian processes and the formation of numerous microfacies environments which manifest in a wide variety of sedimentational structures. Thus, the drying of windward dune slopes always occurs before that of slip face slopes. Consequently, when the former already begin to be actively impacted by wind deflation, the latter remain in a humid state for some

time. In such cases polygenetic types of structures form, for example, *adhesion grain-fall lamination*, etc. [Kasse, Aalbersberg, 2019].

Adhesion structures are identified in large amounts in Late Quaternary aeolian and alluvial-aeolian deposits of Eastern Europe (European Sand Belt), the formation of which is linked to an extremely unstable specific regime of periglacial zone rivers and syngenetic aeolian processing of alluvial deposits [Kasse, 2002; Zieliński et al., 2015; Kasse, Aalbersberg, 2019]. It has been noted that during cryochrones, under conditions of weak surface runoff and excess fine disperse particle sedimentation, the absence of wood vegetation in valleys, watercourse beds were extremely volatile and constantly shallowed and branched out. Bed and floodplain alluvium facies underwent intense aeolian processing during continuous low-water periods.

Recently, widespread Late Pleistocene and Holocene alluvial-aeolian deposits containing buried Belling-Allered soil horizons (14.0–12.2 ka) have been noted in Western Siberia [Zykina et al., 2017; Konstantinov et al., 2019]. It is notable that these soil horizons, which are regional stratigraphic markers, are overlapped by dune deposits of the Younger Dryas.

**Seasonal and perennial cyclical stratification** of dune deposits is related to significant differences in the rate and mechanism of aeolian sedimentation in warm and cold times of the year, seasonal and quasi-periodic climatic processes. Among these are seasonal freezing-thawing of dune surfaces, snow cover, snowfields, flooding of interdune depressions as a result of fluctuations in the level of supra-permafrost waters, short-term fixing of dune surfaces by vegetation.

In some sections of dune deposits the cyclicity of aeolian sedimentation manifests in the interchange of sand series with various sets of specific types of stratification and lamination. Among them, cryogenic-aeolian and niveo-aeolian stratification typical for dune deposits in cold regions should be noted.

*Cryogenic-aeolian seasonal stratification* was first described within one of the largest dune massifs of Kobuk (northwestern Alaska) by E.A. Koster and J.W. Dijkmans [Koster, Dijkmans, 1988]. As a result of year-round observations of the nature of aeolian deposition it was established that at the beginning of the winter period there is dune surface adfreezing, snow cover formation, and an almost complete termination of deflation and accumulation. During the winter period intense redistribution of the snow cover and its partial sublimation lead to the exposure of significant areas of the dunes. Adhering and adfreezing atmospheric dust deposits onto the dune surface as a thin dusty interlayer.

During the summer period the dune surfaces thaws, aeolian activity intensifies, and the accumulation of a new sand layer occurs. This process repeats

year after year and leads to the formation of specific annual cyclicity, which is reasonable to name *cryogenic-aeolian stratification* [Koster, Dijkmans, 1988]. Morphologically similar types of cyclical stratification have been noted in the sand dunes of Soviet Central Asia in the works of A.F. Ivchenko (as cited in [Botvinkina, 1962]).

The works of N.A. Kulik [1928] point to the specific conditions of aeolian deposition in cold regions (Pechorskaya Lowland). The author notes that, unlike deserts in cold and temperate latitudes, here there is a specific mechanism of cryogenic fixing of dune massifs by way of their syngenetic freezing and climbing movement of the active layer bottom syngenetically with aeolian accumulation.

Thin (0.5–1.0 mm) systematic colmatage films of dark dust are found quite often in D'olkuminskaya Series sections (Fig. 10, *a, d*) and match descriptions of the cryogenic-aeolian stratification of the Kobuk massif [Koster, Dijkmans, 1988]. They also match translent pseudo-stratification, but, unlike it, are composed not of a heavy (magnetite), but of a thin and light (dusty) fraction and often include a mix of fine vegetation remains, plant seeds, and microcoals. The mineralogical analysis shows that the dust which forms these films is rich in hydrocarbonates and iron hydroxides. Near the dune surface the films gradually oxidize and obtain a bright ochre color.

The films are even, abrupt, but are much less steady and, unlike translent stratification, often branch out. The distance between neighboring films defines the annual stratification interval of dune sands, which changes from a few millimeters to 10–15 cm and more. The aggregate of the films dividing the broad, light layers is resemblant of the annual growth rings of trees.

Overall, by its formation mechanism the cryogenic-aeolian stratification is related to adhesion stratification. The difference is that the former forms during the cold time of the year, when the dune surface is frozen, and deposition of dusty particles occurs by way of their freezing to the sedimentation surface. The latter forms during the warm time, when the dune surface is melted, deposition occurs by way of adhesion of particles to the humid surface.

*Niveo-aeolian seasonal stratification* is an important diagnostic indicator of aeolian deposits in cold regions. Its formation relates to the burial of winter snow cover in dune sand fragments and its subsequent recrystallization into thin horizontal schlieren of sedimentary-metamorphic (atmospheric) ice [Dijkmans et al., 1986, 1988; Koster, Dijkmans, 1988; Brookfield, 2011; Dinwiddie et al., 2012].

Modern niveo-aeolian formations composed of thin interlayering of sand, loamy sand, and firn (total ice content 40–50 %) were found in the dunes of the dry valley of Victoria in Antarctica [Cailleux, 1974;

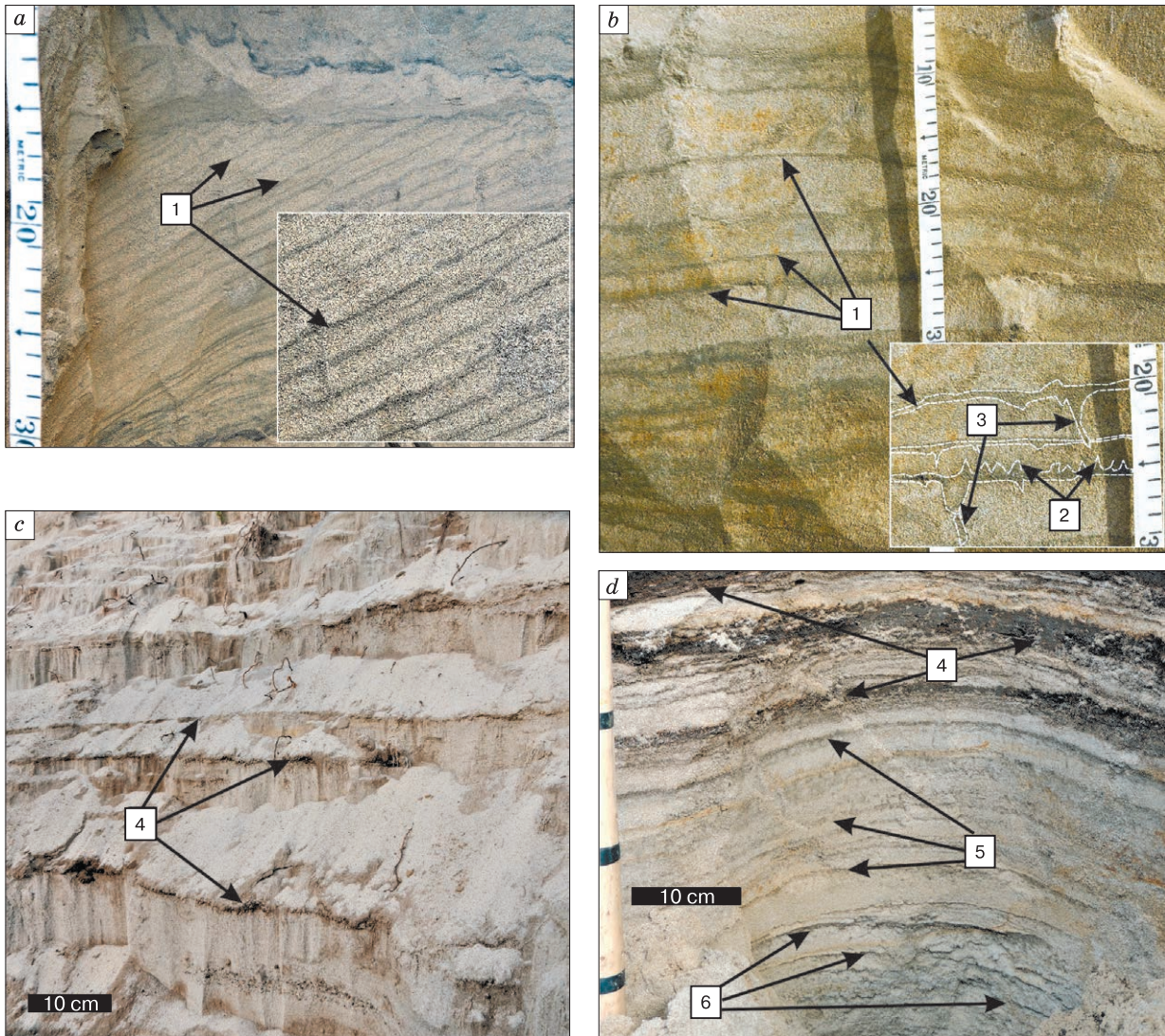


**Fig. 10. Some types of cyclical stratification of D'olkuminskaya Series cover sands in key outcrops in Central Yakutia.**

*a* – inclined cryogenic-aeolian; *b* – gently sloping niveo-aeolian; *c* – biogenic; *d* – primary cryogenic-aeolian and biogenic. 1 – inverse denivational silty interlayers; 2 – vertical inverse small wedges and apophyses; 3 – funnels of vertical drainage of meltwaters; 4 – peat-humus interlayers (paleosols); 5 – denivational colmatage interlayers; 6 – syngenetic schlieren and interlayers of fossil depositionally metamorphic ice. A.A. Galanin's photo from 2015–2019.

*Calkin, Rutford, 1974; Ayling, McGowan, 2006*]. The thickness of individual firm interlayers varies from 1 mm to 4–6 cm, some reach a thickness of 10 cm and more. Systematic burial of the snow cover in sand dune deposits occurs here under conditions of low summer temperatures (near 0 °C and lower) as a result of syngenetic freezing of deposits and continuous upward movement of the bottom of the active layer. Snow cover layers buried in the dune sands subsequently become denser and transform into ground ice schlieren lying either horizontally or at an angle, but parallel to the deposition surfaces.

Primary niveo-aeolian structures are seldom seen in sections in more moderate climates because the seasonal snow cover, including buried snow patches, has enough time to completely melt during the warm time of the year. As a result of permafrost degradation primary niveo-aeolian deposits melt, which leads to the formation of specific denivation structures.

*Denivation structures* form as a result of the melting of the seasonal snow cover. Atmospheric dust, sand, and fine organic detritus which accumulate in them deposit onto the dune surface as a thin (0.5–

4.0 mm) crinkly inversive dark-coloured warp called the denivational interlayer [Dijkmans *et al.*, 1988; Dinwiddie *et al.*, 2012].

Denivation structures also include specific types of stratification related to the melting of ancient niveo-aeolian deposits which contain interlayers and schlieren of fossil firn-ice of sedimentary genesis. The denivation structures manifest as crinkly silt interlayers with distinctive vertical micro-wedge-like apophyses and protuberances, vertical filtration funnels of meltwater, etc. Melting of niveo-aeolian deposits with a high ice content is frequently accompanied by complex microfolding, microsubsidence, fractures, and other types of deformations [Dijkmans *et al.*, 1988].

J.W. Dijkmans and colleagues [Dijkmans *et al.*, 1988] observed melting snow and summer rain waters which flow into enclosed interdune depressions and form microdeluvial, microproluvial facies, as well as inner microdeltas composed of thin denivational warp layers on the Kobuk dune massif. Because of high hygroscopy and poor permeability the denivation interlayers make meltwater and rainwater drainage difficult, which leads to permafrost aggradation, an increase in the permafrost aquitard, and an even higher seasonal flooding of interdune depressions. Denivation stratification is vastly represented in D'olkuminskaya Series deposits in many outcrops of Central Yakutia (Fig. 10, *b, d*).

Ultimately, the freezing of interdune basins floors and the increase in atmospheric precipitation on the border of the Neopleistocene and Holocene led to the formation of numerous shallow ephemeral water pools in which there was an accumulation of aeolian-lake deposits first, then swamp deposits. Such formations are widespread in the top of the D'olkuminskaya Series and are identified in the top part of the Peschanaya Gora outcrop (unit IV). They formed during the first half of the Holocene during the beginning stages of fixing of Younger Dryas dunes of the Kerdyom and Bestyakh terraces of the Lena River.

Many researchers [Kasse, 2002; Zieliński *et al.*, 2015; Kasse, Aalbersberg, 2019] captured the wide distribution of niveo-aeolian and denivation structures in the aeolian deposits of the last cryochrone (MIS-2) within the periglacial European Sand Belt. Analogous structures are identified in aeolian sand covers within North American cryolithozones [Koster, Dijkmans, 1988; Ayling, McGowan, 2006; Dinwiddie *et al.*, 2012].

*Biogenic-aeolian cyclical stratification* is found in some D'olkuminskaya Series outcrops. It is composed of systematically interchanging thin, parallel, divot-loamy sand interlayers 3–5 mm thick and layers of bleached quartz sand from 2–3 to 10–15 cm thick. The stratification origin is related to short episodes of fixing of sand dune surfaces by grass vegetation. On

individual parts of the D'olkuminskaya Series territory, especially near its top, units with dozens of divot laminae (Fig. 10, *c, d*) which include buried grass tussocks, can be observed.

*Biogenic-aeolian humus veins and nodules* are widespread near the top of the D'olkuminskaya Series and reach 1.5–2.0 m in width and 0.5–1.5 m in thickness (Fig. 11). These veins form at the stage of fading aeolian activity, when a curtain herbaceous cover consisting of dense sedge-cereal tussocks forms on the dune surface. Continuous accumulation of new sand layers leads to a rise in the dune surfaces and depresses lateral tussock growth, as a result of which they continuously grow upward (Fig. 11, *b*). The grassy organic material of the tussocks decomposes quite quickly, which leads to the formation of isolated intensely humified spots, nodules, and diversely shaped veins. In more humid areas, because of high hygroscopy, the humus veins begin to freeze intensely with the formation of massive ice-ground veins (Fig. 11, *d*).

**Cryogenic structures and textures** in the D'olkuminskaya Series dune deposits is significantly diverse, but does not reach a large scale compared to the ice-loess covers of the Yedomia Series. The content of cementing porous ice varies from 5 to 30 % [Galanin *et al.*, 2018]. “Sublimational” cryostructures represented by hoar-ice on grain contacts, thin ice films, and schlieren are more frequent in frozen sands which are extremely undersaturated with water. Massive cryotextures, the formation of which is related to the freezing of vertical and horizontal ground water infiltration zones, are often seen near the bottom of the series.

M.S. Ivanov [1984] points out that within the Peschanaya Gora outcrop he has discovered interlayers, schlieren, and fossil ice deposits from several millimeters to 3–4 meters thick. The majority of ground ice is concentrated in inclined bedding facies. Ice interlayer orientation repeats the stratification of enclosing dune deposits, based on which a sedimentary-metamorphic (atmosphere) origin of this ice by way of recrystallization of buried snow patches can be assumed.

V.B. Spektor and colleagues [2011] also point out the presence of fossil ice strata of firn origin in the Yedomia Series deposits of the Lena-Amga interfluvium. According to the authors, the main indicators of their formation are strata type deposits, thin horizontal and wavy stratification, a light isotope composition ( $\delta^{18}\text{O} = -30.8 \pm 0.9 \text{‰}$ ;  $\text{D} = -227.9 \pm 6.9 \text{‰}$ ), and the presence of a significant amount of cryophytic herbaceous vegetation pollen.

Secondary sand veins and small wedges and pseudomorphs after PIW are usually linked to buried soil horizons in the bottom and top of the D'olkuminskaya Series, as well as buried Belling-Allered soils. These formations have an epigenetic origin related to episodes of soil-vegetative cover fixing of dunes, in-

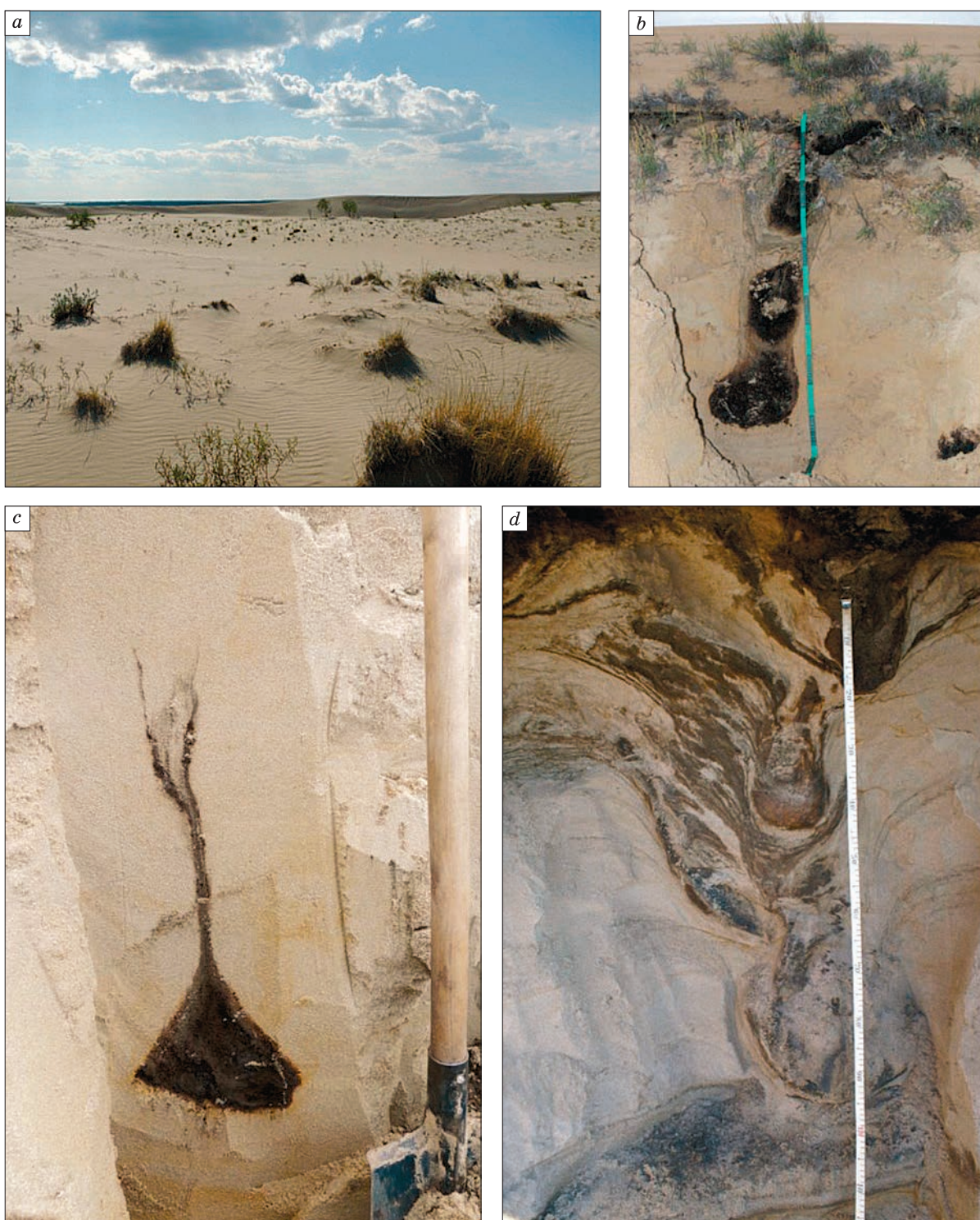


**Fig. 11. Holocene biogenic-aeolian humus veins and nodules in D'olkuminskaya Series dune deposits (Kysyl-Syr outcrop in the basin of the lower course of the Vilyuy River, Central Yakutia).**

*a* – stage of partial fixing of dunes by herbaceous tussocks; *b* – “migrating” humus nodules under a modern tussock; *c* – fully humified herbaceous tussock in dune sands; *d* – ice humus-sandy vein in frozen dune sands. A.A. Galanin's photo from July, 2015.

tense freezing, and an increased permafrost aquitard. Signs of cryoturbational processes in the form of microfolding are often seen in the same horizons.

### **Peschanaya Gora facies composition and age**

Bestyakh Series pebble-gravel-sand deposits (units Ia, Ib) lying at the very base of the Kerdyom 25-meter terrace and categorized as Middle Neopleistocene “periglacial alluvium” by predecessors (bs Q<sub>II</sub>) [Alekseev et al., 1990; Kamaletdinov, Minuk, 1991] are among the oldest formations. As of yet there are no absolute dates for the Bestyakh Series. The series’ reverse magnetization identified in the Peschanaya Gora outcrop has been juxtaposed to the Matuyama Chron, the upper boundary of which is 780 ka [Kamaletdinov, Minuk, 1991; Minuk, 2004]. At the same time, the age of the alluvium at the bottom of Peschnaya Gora can be juxtaposed to the Blake or Seroglazka magnetic events (100 and 120 ka), especially considering that these events have already been identified in the sections of some terraces of Central Yakutia [Minuk, 2004].

The author of the present study has established a small-thickness sand unit (unit II) above the Bestyakh Series, possibly linked by predecessors to the “periglacial alluvium” of the Middle Pleistocene-aged Mavrinskaya Series (mv Q<sub>II–III</sub>) [Alekseev et al., 1990; Kamaletdinov, Minuk, 1991; Spektor et al., 2017].

Because of a significant structural non-homogeneity, for convenience of research in the present article unit II has been divided into four nominal units (IIa–IIId), which differ significantly in their sedimentary stratification and lamination features. The bottom unit IIa has clear signs of alluvial origin in the form of oblique series of submarine dunes and riffles.

The overlaying unit IIb is composed predominantly of humid aeolian deposit structures: wavy adhesion stratification and lamination types, as well as niveo-aeolian and denivation structures. The given facies set is typical for vast point bars, sandspits, and low basins with a rather sparse grass-subshrub cover, which are flooded rarely and for short periods of time during the spring snowmelt. The date obtained for the root of unit IIb (at a depth of 20 m from the brink of the terrace and 5 meters above the Lena River edge) – 22.10–19.60 ka (MPI-759) [Alekseev et al., 1990] – indicates deposit formation during the thermal minimum of MIS-2.

Unit IIc contains structures of dry aeolian deposition represented by translant stratification and climbing ripple lamination, as well as deflational horizons with fine gravel and fragments of poorly developed paleosols. The age of the latter (unit IIId) is characterized by two dates: 18.39–16.70 ka (MPI-901) at a depth of 15 m [Kamaletdinov, Minuk, 1991] and 18.33–15.68 ka (MPI-760) at a depth of 14 m [Alekseev et al., 1990].

Overall, the stratigraphic sequence of the facies of units IIa–IIc indicates a continuous decrease in the amount of atmospheric precipitation, a decrease in surface runoff, and an increase in aeolian process activity in the first half of MIS-2.

A wide distribution of deflational horizons in unit IIc and thin horizontal paleosol interlayers (unit IIId) indicates that during this period the valley of the Lena River was a long deflational basin from which alluvial sediments were carried by wind in a southeast direction and partially deposited within the Kerdyom terrace. The bottom of the Paleo-Lena basin during this period was possibly a cold sand-gravel semidesert discontinuously covered with grass-subshrub vegetation. Secondary sand veins and wedges indicate an intense freezing of aeolian sand deposits under conditions of severe dehydration. Paleo-Lena runoff and the volume of annual river loads in this period were very insignificant.

Unit IIIa deposits differ drastically from underlying deposits. Structures of fast accumulation of aeolian deposits under dry conditions formed by gently sloping windward and steep dune slip face and crest facies dominate here. The former are represented by translant climbing ripple stratification, the latter by steeply inclined grain-fall dune slip face structures. Sediment bedding and lamination indicate aeolian transport in a southeast direction, opposite the modern flow of the Lena River.

11 m below the terrace brink (14 m above the Lena’s water level) a date of 14.07–13.40 ka (GIN-2461) [Kamaletdinov, Minuk, 1991] was obtained from a paleosol fragment (unit IIIb), which matches the Belling–Allerød warming. Due to this it can be assumed that the formation of unit IIIa took place during the interval 17.00–14.00 ka. The Lena’s valley bottom in this period was covered with parabolic and spear-shaped dunes of a southeast orientation. The absence of adhesion, niveo-aeolian, and denivation structures in unit IIIa indicates hyperarid conditions, an extremely small amount of atmospheric precipitation, a lack of a snow cover or its insignificant role. At the same time, fading deflation and an increase in the rate of aeolian accumulation within the Kerdyom terrace and Central Yakutia in general indirectly indicates an influx of new aeolian loads and an increase in river runoff in the interval of 15–14 ka. An increase in runoff and the volume of river loads may be related to the beginning of the degradation of the last mountain glaciation in the Paleo-Lena basin.

The Unit IIIc, overlapping the Belling–Allerød paleosol, is similar to unit IIIa in terms of facies. Swift dry aeolian deposition structures (translant climbing ripple lamination, grain-fall lamination) are predominant here. Horizontal and wavy types of aeolian stratification are spread through the top portion of the unit, biogenic stratification in the form of tiers of thin divot interlayers appears. Adhesion and niveo-

aeolian stratification types and denivation structures appear near depressions of the unit top, which indicates an increase in the influence of the snow cover. The formation of unit IIIc is related to the last pulse of the Younger Dryas global cooling, which is clearly reconstructed in all Late Neopleistocene aeolian covers of Northern Eurasia [Kasse, 2002; Zieliński, 2015; Zykina et al., 2017; Kasse, Aalbersberg, 2019; Konstantinov et al., 2019].

Unit IV deposits form a gently sloping depression on the top of the D'olkuminskaya Series, which is filled with lake and swamp deposits. In the bottom portion (unit IVa) there are facies of a small body of water which appeared in an enclosed interdune basin on the border of the Neopleistocene and Holocene. Contrasting interchange of greyish lake loamy sands and well sorted white aeolian sands (unit IVb) indicate a periodic drying out of the lake. Clearly, the lake existed at this site for a very short time and quickly filled with deposits, of which there was an abundant influx from nearby unvegetated dunes.

During the Early Holocene a peat bog (unit IVc) appeared in place of the lake and persisted through the Middle Holocene. Several radiocarbon dates indicate the age of the peat bog. At a depth of 2.4 m from the surface (unit IVc) a date of 8.99–8.60 ka (GIN-2462) was obtained [Alekseev et al., 1990]. The author of the present article obtained four more dates for unit IVc from depths of 2.5, 2.0, 1.5, and 1.0 m: 9.89–8.58 ka (MPI-121), 8.06–6.72 ka (MPI-118), 12.03–9.89 ka (MPI-119), and 7.86–6.65 ka (MPI-120), respectively. The obtained dates have a certain inversion, but definitely indicate a fast accumulation of the peat bog over the course of the first half of the Holocene in the interval from 10 to 6 ka.

The author has established numerous freshwater mollusk and ostracod shells from 1 to 4 mm in size in the top of the lake deposits. According to the data of V.A. Kamaletdinov and P.S. Minuk [1991], they are represented by a set of species which are widely distributed in modern shallow brackish lakes of Central Yakutia.

It is imperative to note that systematic interlayers of well-sorted white quartz sand are present in the bottom layers of the peat unit, and they are completely absent in the top layers. This indicates that during the beginning period of its formation this and other peat bogs were small vegetation oases within a wide field of unvegetated U-shaped dunes of the Kerdyom terrace. Complete stabilization of the latter with vegetation had clearly finished by the beginning of the Boreal optimum of the Holocene, since the middle and top parts of the peat layers have no mineral interlayers.

#### **Pollen and paleontological composition of aeolian sand covers of Central Yakutia**

*The spore-pollen composition* of the D'olkuminskaya Series is known by individual samples and is

rather scant. According to the data of V.V. Spektor and colleagues [2017], spores and pollen in the Peschanaya Gora outcrop are predominantly represented by herbaceous taxa and contain a significant amount of mineralized, mechanically damaged, and redeposited grains. The pollen composition indicates formation of the D'olkuminskaya Series under conditions of a discontinuous soil-vegetation cover of impoverished steppes where xerophytic taxa dominated: Artemisia, Poaceae, sedges, Caryophyllaceae, and Chenopodioideae (Artemisia, Cyperaceae, Asteraceae, Chenopodiaceae, Poaceae, Ranunculaceae, Fabaceae, Brassicaceae). A small presence of tree, shrub and subshrub pollen (*Pinus*, *Larix*, *Betula*, *Alnaster*, *Ericales*, *Selaginella* sp.), as well as moss spores (*Sphagnum*) and seaweed (*Botryococcus*), indicates a mosaic landscape in which small bodies of water and possible wood-shrub vegetation oases persisted.

Similar pollen spectrums are established in D'olkuminskaya Series sections in a 45-meter (Bestyakh) terrace of the Lena River near the small town of Nizhny Bestyakh [Pravkin et al., 2018], 120 km south of Peschanaya Gora, in a 12-meter terrace of the Suola River (right-bank tributary of the Lena River [Potapova et al., 2016], as well as in a 35-meter terrace of the Vilyuy River [Pavlova et al., 2017; Galanin, Pavlova, 2019]. An additional feature of the series is the vastitude of *Glomus* and *Sordaria* spores, which live on the excrements of large herbivores and are typical for dry landscapes with discontinuous soil-vegetation cover [Potapova et al., 2016].

*The paleontological composition* of the D'olkuminskaya Series can be described using the example of the Suullar Myraan outcrop (62°33.54' N; 129°59.49' E) on the right bank of the Lena River, 20 km downstream of the Kangalassky cape, as well as in the Megin mammoth fauna location in the river cliff of a 12-meter terrace of the Suola River (62°05.14' N; 130°11.18' E), situated within the dune cover distribution of the D'olkuminskaya Series (Fig. 4). *Mammuthus primigenius*, *Bison priscus*, *Coelodonta antiquitatis*, *Equus lenensis*, *Saiga tatarica* remains are identified in the Suullar Myraan outcrop (Kerdyom terrace of the Lena River) [Spektor et al., 2017]. A date of 23.79–21.86 ka (GIN-14410) [Spektor et al., 2017] has been obtained for the bone of a woolly rhinoceros, which corresponds to the beginning of MIS-2.

60 fauna and 25 vegetation taxa were identified in the peat bog of the Megin outcrop based on carpological analysis [Potapova et al., 2016]. The remains of several *Bison priscus*, *Ovibos moschatus*, *Equus lenensis* individuals and an almost complete skeleton of an archaic form of *Mammuthus primigenius* (*Megin Mammoth*) were identified, the calibrated age of the latter of which – 23.86–22.65 ka (MPI-80) – is also associated with the beginning of MIS-2. A paleoecological reconstruction of the flora and fauna of the

peat bog has revealed that during its formation the average temperature in July was no less than +12 °C. The vegetation cover was formed by a mosaic combination of impoverished steppes, meadows, islands of larch forests and vast unvegetated landscapes [Potapova *et al.*, 2016]. Remains of aquatic vegetation together with xerophytes indicate significant seasonal fluctuations in the level of bodies of water and the domination of evaporative environments.

It must be noted that all the numerous discoveries of large herbivores of the mammoth biome in Central Yakutia date to the Kargin thermochrone (MIS-3) [Boeskorov *et al.*, 2016]. Currently all discoveries of later representatives of the mammoth biome of Central Yakutia (Megin mammoth – 23.86–22.65 ka; Suolsky mammoth – 22.06–21.45 ka; woolly rhinoceros from the Suullar Myraan section – 23.79–21.86 ka) are limited to the beginning of MIS-2. All the aforementioned discoveries are associated with the bottom of the D'olkuminskaya Series; they are not found within the series itself. Results of studies of the D'olkuminskaya Series key sections have demonstrated that a catastrophic drought and desertification of Central Yakutia started at the beginning of MIS-2 and peaked in the interval of 18–13 ka. The maximum expansion of dune cover areas happened specifically during this time, and likely a sharp decline in the areas and productivity of meadow steppes – the main feed base of the mammoth biome.

It is curious that later and seemingly already disappearing Suolsky and Meginsky mammoths are associated with the archaic form, which is morphologically cognate with the steppe mammoth [Boeskorov, Mashchenko, 2014]. It is possible that these forms were the last micropopulations which inhabited small oases of vegetation among surrounding D'olkuminskaya Series dune covers and attempted to adapt to the conditions of extreme drought and desertification. Indeed, the disappearance of the larger representatives of the mammoth biome of Central Yakutia 10–12 thousand years earlier, compared to more northern and eastern regions, is difficult to relate to warming climate in the Holocene. But it can be explained by desertification, expansion of the area of dune massifs, a decrease in Yedomas meadow steppe areas and productivity – the main feed base of the mammoth biome. Of course, this assumption requires additional factual justification.

## CONCLUSION

The results of the additional study of the Peschanaya Gora key outcrop and other sections of Central Yakutia indicate a subaerial origin of D'olkuminskaya Series cover sands in cold and dry conditions of the final Neopleistocene. The majority of its facies features are typical for contemporary and Late Quaternary dune massifs which are widely distributed in the

cold regions of North America, Europe, Western Siberia.

A revision of radiocarbon datings of all key sections of Central Yakutia shows that the main portion of the D'olkuminskaya Series within the Kerdyom 25-meter terrace formed in the interval from 22 to 12 ka. In the interval of 22–17 ka (thermic minimum of MIS-2), because of a catastrophic decrease in the amount of precipitation and river runoff, a deflationary basin partially fixed by certain herbaceous vegetation formed within the bottom of the valley of Paleo-Lena. The majority of river channel and basin deposits was carried away beyond the basin in a southeast direction and deposited within the Kerdyom and Bestyakh terraces.

In the interval of 17–14 ka deflation was replaced by intense aeolian accumulation, as a result of which a sand dune desert with islands of tundra-steppe vegetation formed within the Kerdyom and Bestyakh terraces of the Lena River.

In the interval of 14–13 ka dune relief stabilization of the Kerdyom and Bestyakh terraces by grass-subshrub xerophytic groups and islands of wood vegetation was taking place under conditions of climate softening (Belling-Allerød warming).

In the interval of 12.8–11.8 ka there was abrupt Younger Dryas desertification, which was accompanied by the expansion of dune massifs within the Kerdyom and Bestyakh terraces of the Lena River.

During the beginning of the Holocene in the interval of 11–10 ka, as a result of a significant increase in atmospheric precipitation and climate softening, the surface of the dunes began to gradually become colonized by vegetation. At the initial stage many shallow lakes were formed in enclosed interdune depressions, the smaller of which became swamps with abundant peat accumulation by the beginning of the Boreal optimum of the Holocene. The final stabilization of the Kerdyom terrace dune relief by vegetation ended approximately 9–8 ka.

The mineralogical similarities between dune (D'olkuminskaya Series), loess-ice (Yedomas Series), and alluvial deposits in the basin of the middle course of the Lena River indicate a common source of terrigenous material (Jurassic greywacke-quartz sandstone). An important indicator of the aeolian origin of D'olkuminskaya Series dune deposits is an almost threefold increase in the content of the heavy fraction and magnetite to 3.1 % in comparison to the underlying alluvium of the Bestyakh (1 %) and Mavrinskaya (1.1 %) series. Another important mineralogical indicator is the presence of secondary carbonate and metal hydroxide in dune deposits, which form specific cementing films and interlayers called calcretes.

The features of the granulometric composition and mineralogical similarities of the D'olkuminskaya and Yedomas series indicate that they are two separate granulometric derivatives which appeared as a result

of aeolian differentiation of a single source – Quaternary alluvium of the Bestyakh and Mavrinskaya series. The first derivative (dune sands) consists predominantly of sand fractions, and the latter (loess) of dusty fractions. This conclusion proves the zonal character of the spatial distribution of dune massifs and loess-like deposits in relation to the east-south-east direction of wind transfer in the region. As such, the D'olkuminskaya Series dune deposits compose predominantly the 18–25-meter (Kerdyom) and 45–75-meter (Bestyakh) terraces of the Lena River, while the main area of the ice-loess covers of the Yedoma Series is located eastward and linked to higher elements of the Lena-Amga interfluvial relief (Tyungulu, Abalakh, and Magan surfaces).

The sedimentational structure of the D'olkuminskaya Series deposits is represented by a wide set of specific types of stratification and lamination, some of which are typical only for aeolian deposits. They include translational climbing ripple stratification and lamination, grain-fall cross-stratification and lamination of steep dune slip faces and others.

The formation of the D'olkuminskaya Series in cold arid conditions is emphasized by the wide distribution of primary sandy veins and wedges and other structures of dry aeolian deposition. Additionally, adhesion, niveo-aeolian and denivation structures formed under conditions of seasonal snow cover and contrasting humidification are widespread in the composition of its individual units in the bottom and top.

An analysis of pollen and paleontological data shows that the cooling and desertification of the last cryochrome (MIS-2), which took place in the interval of 22–17 ka, was catastrophic in Central Yakutia and could have been the cause of the early extinction of some of the larger representatives of the mammoth biome.

**Acknowledgements.** *The author would like to thank the staff of MPI SB RAS I.V. Klimova, G.I. Shaposhnikova, A.L. Lobanova, N.N. Remizova, A.N. Vasilieva, and A.M. Safina for their help in the completion of analyses.*

*The study was conducted with support from RFBR No. 17-05-00954-a, RFBR-RS(Y) No. 15-45-05129, No. 18-45-140012.*

## References

- Alekseev, M.N., 1961. Stratigraphy of continental Neogene and Quaternary deposits of the Vilyuy depression and the valley of the lower reaches of the Lena River. USSR Academy of Sciences, Moscow, 120 pp. (in Russian).
- Alekseev, M.N., Grinenko, O.V., Kamaletdinov, V.A., et al., 1990. Neogene and Quaternary deposits of the Lower Aldan depression and the Middle Lena (Central Yakutia). Geological excursion guide. YSC SO AN SSSR, Yakutsk, 42 pp. (in Russian).
- Alekseev, M.N., Kamaletdinov, V.A., Grinenko, O.V., 1984. Cenozoic deposits of the Lena and Aldan. In: 27<sup>th</sup> International Geological Congress. Yakut ASSR, Siberian platform. Generalized guide of excursions 052, 053, 054, 055. Nauka, Novosibirsk, pp. 21–42 (in Russian and in English).
- Astakhov, V.I., Svensen, J.I., 2011. Covering formation of the Final Pleistocene in the extreme north-east of European Russia. Regional'naya geologiya i metallogeniya [Regional Geology and Metallogeny], No. 47, 12–27 (in Russian).
- Ayling, B.F., McGowan, H.A., 2006. Niveo-aeolian Sediment Deposits in Coastal South Victoria Land, Antarctica: Indicators of Regional Variability in Weather and Climate. Arctic, Antarctic, and Alpine Research 38 (3), 313–324.
- Black, R.F., 1951. Eolian deposits of Alaska. Arctic 4 (2), 89–111.
- Blott, S.J., Pye, K., 2001. Gradistat: a grain size distribution and statistics package for the analysis of unconsolidated sediments. Earth Surface Processes and Landforms, vol. 26, 1237–1248.
- Boeskorov, G.G., Mashchenko, E.N., 2014. The systematic position of the “Suolsky” mammoth (Mammuthus, Proboscidea). Nauka i obrazovanie [Science and Education], No. 2, 48–54 (in Russian).
- Boeskorov, G.G., Nogovitsyn, P.R., Mashchenko, E.N., et al., 2016. New data on mammals of the mammoth fauna of the Middle Lena Basin (Yakutia; the national natural park “Lena Pillars” and adjacent territories). Doklady Akademii Nauk [Reports of the Academy of Sciences], 469 (2), 190–194, DOI: 10.7868/S0869565216200147.
- Boggs, Jr.S., 2009. Sedimentary structures. In: Petrology of Sedimentary Rocks. Cambridge University Press, Cambridge, pp. 63–110.
- Bolshiyarov, D.Yu., Makarov, A.S., Schneider, V., et al., 2013. Origin and Development of the Lena River Delta. AARI, St. Petersburg, 268 pp. (in Russian).
- Bolshiyarov, D.Yu., Tide, Y., Savelieva, L.A., et al., 2016. To the study of the stages of development of the river valley Lena. In: Proceedings of the All-Russian Scientific and Practical Conference “Geology and mineral resources of the North-East of Russia” (Yakutsk, April 6–8, 2016). NEFU, Yakutsk, pp. 469–472 (in Russian).
- Botvinkina, L.N., 1962. Layering of sedimentary rocks. In: Proceedings of the Geological Institute of the USSR Academy of Sciences. USSR Academy of Sciences, Moscow, vol. 51, 542 pp. (in Russian).
- Bronk, R.C., 2009. Bayesian analysis of radiocarbon dates. Radiocarbon, No. 51 (1), 337–360.
- Brookfield, M.E., 2011. Aeolian processes and features in cool climates. Geological Society London Special Publications, pp. 241–258.
- Cailleux, A., 1974. Formes précoces et albédos du nivéo-éolien. Z. Geomorphology, No. 18, 437–459.
- Calkin, R.E., Rutford, R.H., 1974. The Sand Dunes of Victoria Valley, Antarctica. Geographical Review 64 (2), 189–216.
- Caputo, M., 2020. Adhesion Ripple Structures in Quaternary Carbonate Eolianites, San Salvador Island, the Bahamas. Preprint, 13 pp.
- Carter, L.D., 1981. A Pleistocene Sand Sea on the Alaskan Arctic Coastal Plain. USGS Staff Published Research 924.
- Derbyshire, E., Owen, L.A., 2017. Glacioaeolian processes, sediments, and landforms. In: Past Glacial Environments. J. Menzies, J. van der Meer (Eds.). Elsevier, N.Y., pp. 273–308.

- Dijkmans, J.W.A., Galloway, J.P., Koster, E.A., 1988. Grain-size and mineralogy of eolian and fluvial sediments in the central Kobuk valley, northwestern Alaska. Department of the interior United States Geological Survey. Open-file report No. 88-369, 21 pp.
- Dijkmans, J.W.A., Koster, E.A., Galloway, J.P., et al., 1986. Characteristics and origin of calcretes in a subarctic environment. Great Kobuk Sand Dunes, northwestern Alaska, USA. *Arctic and Alpine Research* 18, 377–387.
- Dinwiddie, C.L., McGinnis, R.N., Stillman, D.E., et al., 2012. Internal sedimentary structure and aqueous-phase distribution of the Great Kobuk Sand Dunes, northwestern Alaska: Insights from an arctic aeolian analog site. In: *Third International Planetary Dunes Workshop: Remote Sensing and Image Analysis of Planetary Dunes*. USA, Arizona, Flagstaff, 2012 June 12–15, abstract #7034. – <https://www.lpi.usra.edu/meetings/dunes2012/pdf/7034.pdf>
- Ershov, E.D., 1989. *Geocryology of USSR*. Middle Siberia. Nedra, Moscow, 414 pp. (in Russian).
- Fedorovich, B.A., 1983. Zonality of aeolian relief formation. In: *Dynamics and patterns of relief formation of deserts*. Nauka, Moscow, 236 pp. (in Russian).
- Fenton, L.K., Hayward, R.K., Horgan, B.H.N., et al., 2013. Summary of the Third International Planetary Dunes Workshop: Remote Sensing and Image Analysis of Planetary Dunes, Flagstaff, Arizona, USA, June 12–15, 2012. *Aeolian Research*, No. 8, 29–38.
- Filippov, V.Ye., Vasiliev, I.S., 2006. Periglacial relief of the Lena-Vilyuy interfluvium. *Geografiya i prirodnye resursy* [Geography and Natural Resources], No. 4, 82–86.
- Folk, R.L., 1980. *Petrology of sedimentary rocks*. Texas, Hemphill Publishing Company Austin, 350 p.
- Galanin, A.A., Pavlova, M.R., Klimova, I.V., 2018. Late Quaternary dune formations (D'olkuminskaya Series) in Central Yakutia (Part 1). *Earth's Cryosphere*, XXII (6), 3–14.
- Galanin, A.A., Pavlova, M.R., 2019. Late Quaternary dune formations (D'olkuminskaya Series) in Central Yakutia (Part 2). *Earth's Cryosphere*, XXIII (1), 3–15.
- Galanin, A.A., Pavlova, M.R., Shaposhnikov, G.I., Lytkin, V.M., 2016. Tukulans: sand deserts of Yakutia. *Priroda* [Nature], No. 11, 44–55.
- GOST 12536-2014. *Soils. Methods of laboratory determination of granulometric (granular) and microaggregate composition*, 2015. Staidartinform, Moscow, 18 p. – <http://docs.cntd.ru/document/1200116022>
- Huissteden, J.V., Vandenberghe, J., Van der Hammen, T., Laana, W., 2000. Fluvial and aeolian interaction under permafrost conditions: Weichselian Late Pleniglacial, Twente, eastern Netherlands. *Catena* 40 (3), 307–321.
- Hunter, R.E., 1977. Basic types of stratification in small eolian dunes. *Sedimentology* 24, 361–387.
- Ivanov, A.D., 1966. *Aeolian sands of Western Transbaikalia and the Baikal region*. Buryat. Book Publishing House, Ulan-Ude, 232 pp. (in Russian).
- Ivanov, M.S., 1984. Cryogenic structure of the Quaternary deposits of the Lena-Aldan depression. *Nauka*, Novosibirsk, 126 pp. (in Russian).
- Kamaletdinov, V.A., Minuk, P.S., 1991. Structure and characteristics of sediments of the Bestyakh terrace of the Middle Lena River. *Byulleten' Komissii po izucheniyu chetvertichnogo perioda AN SSSR* [Bulletin of the Commission of Quaternary Research of AS USSR], No. 60, 68–78 (in Russian).
- Kasse, C., 2002. Sandy aeolian deposits and environments and their relation to climate during the Last Glacial Maximum and Lateglacial in northwest and central Europe. *Progress in Physical Geography: Earth and Environment*, No. 26 (4), 507–532.
- Kasse, C., Aalbersberg, G., 2019. A complete Late Weichselian and Holocene record of aeolian coversands, drift sands and soils forced by climate change and human impact, Ossendrecht, the Netherlands. *Netherlands Journal of Geosciences* 98, e4-1–e4-22.
- Kolpakov, V.V., 1983. Aeolian Quaternary deposits in the Lena area of Yakutia. *Byulleten' Komissii po izucheniyu chetvertichnogo perioda AN SSSR* [Bulletin of the Commission of Quaternary Research of AS USSR], No. 52, 123–131.
- Konstantinov, A., Loiko, S., Kurasova, A., et al., 2019. First Findings of Buried Late-Glacial Paleosols within the Dune Fields of the Tomsk Priobye Region (SE Western Siberia, Russia). *Geosciences* 9(82), 1–18.
- Kossovskaya, A.G., 1962. Mineralogy of the terrigenous complex of the Vilyuy Depression and Western Verkhoyansk. *Tr. Geological Institute of the USSR Academy of Sciences*. Issue 63. USSR Academy of Sciences, Moscow, 190 pp. (in Russian).
- Koster, E.A., Dijkmans, J.W.A., 1988. Niveo-aeolian deposits and denivation forms, with special reference to the Great Kobuk Sand Dunes, northwestern Alaska. *Earth Surface Processes and Landforms*, No. 13, 153–170.
- Kulik, N.A., 1928. About the sands of the Pechora region. *Doklady Akademii Nauk* [Reports of the Academy of Sciences]. Ser. A, No. 9, 156–158.
- Kutyrev, E.I., 1968. Formation conditions and interpretation of oblique bedding. *Nedra*, Leningrad, 128 pp. (in Russian).
- Kuznetsova, L.V., Zakharova, V.I., Sosina, N.K., et al., 2010. Flora of Yakutia: geographical and ecological aspects. *Nauka*, Novosibirsk, 192 pp. (in Russian).
- Lea, P.D., 1996. Vertebrate tracks in Pleistocene eolian sand-sheet deposits of Alaska. *Quaternary Research* 45 (2), 226–240.
- Map of Quaternary formations of the territory of the Russian Federation. Scale 1:2 500 000, 2014. VSEGEI. Moscow. Electronic resource on 1 sheet.
- Map of Quaternary Deposits of the USSR, 1959. VSEGEI. Moscow. Electronic resource on 1 sheet. – [http://neotec.ginras.ru/neomaps/M050\\_Union\\_1959\\_Quatern-depos.jpg](http://neotec.ginras.ru/neomaps/M050_Union_1959_Quatern-depos.jpg)
- Map of Quaternary Deposits of the USSR. Scale 1:16 000 000. 1983. In: *Atlas of the USSR*. Main Directorate of Geodesy and Cartography under the Council of Ministers of the USSR, Moscow, pp. 90–91.
- Minuk, P.S., 2004. *Magnetostratigraphy of the Cenozoic of northeastern Russia*. SVKNII FEB RAS, Magadan, 198 pp. (in Russian).
- Okhotin, V. V., 1933. Granulometric classification of soils based on their physical and mechanical properties. *Lengostransizdat*, Leningrad, 70 pp. (in Russian).
- Pavlova, M.R., Rudaya, N.A., Galanin, A.A., et al., 2017. The structure and dynamics of the development of dune massifs of the Vilyuy basin in the Late Quaternary (on the example of the Makhatta and Kysyl-Syr tukulans). *Contemporary Problems of Ecology* 10 (4), 411–422.
- Pewe, T.L., 1975. *Quaternary Geology of Alaska*. United States Government printing office, Washington, 144 pp.
- Pewe, T.L., Journaux, A., 1983. Origin and character of loess-like silt in unglaciated south-central Yakutia, Siberia, U.S.S.R. Geological survey. Professional paper 1262. United States Government Printing Office, Washington, 46 pp.

- Pomortsev, O.A., Bolshiyarov, D.Yu., Popov, V.B., et al., 2017. On the problem of marine transgressions and sedimentary environments in Central and Northern Yakutia in the Neopleistocene. *Vestnik SVFU. Seriya Nauki o Zemle* [Bulletin SVFU. Earth Sciences series], No. 4 (08), 5–13.
- Potapova, O., Maschenko, E.N., Protopopov, A., et al., 2016. The sartzanian biodiversity of Central Yakutia, Russia: the analyses of the new Late Pleistocene Megin Site. Society of Vertebrate Paleontology – 76<sup>th</sup> Annual Meeting, October 26–29, 2016, Salt Lake City, Utah, USA. *Journal of Vertebrate Paleontology, Program and Abstracts*, 208 pp.
- Pravkin, S.A., Bolshiyarov, D.Yu., Pomortsev, O.A., et al., 2018. Relief, structure and age of Quaternary sediments of the river valley. Lena in the Yakutsk bend. *Vestnik Sankt-Petersburgskogo universiteta. Nauki o Zemle* [Bulletin of St. Petersburg University. Earth Sciences], No. 63 (2), 209–229.
- Schwan, J., 1986. The origin of horizontal alternating bedding in Weichselian aeolian sands in Northwestern Europe. *Sedimentary Geology*, No. 49, 73–108.
- Schwan, J., 1988. The structure and genesis of Weichselian to Early Holocene Aeolian sand sheets in western Europe. *Sedimentary Geology* 55, 197–232.
- Siegert, K., Staukh, G., Lemkul, E., et al., 2007. Development of glaciation of the Verkhoyansk ridge and its foothills in the Pleistocene: results of new research. *Regional geology and metallogeny* [Regional Geology and Metallogeny], No. 30–31, 222–228.
- Sizov, O.S., 2015. Geocological aspects of modern aeolian processes in the northern taiga subzone of Western Siberia. Electronic resource. Academic Publishing House “Geo”, Novosibirsk, 124 pp. (in Russian).
- Sizov, O., Konstantinov, A., Volvakh, A., Molodkov, A., 2020. Timing and Sedimentary Record of Late Quaternary Fluvio-Aeolian Successions of the Tura-Pyshma Interfluvium (SW Western Siberia, Russia). *Geosciences* 10 (396), 1–19.
- Soloviev, P.A., 1959. Cryolithozone of the northern part of the Lena-Amga interfluvium. *USSR Academy of Sciences*, Moscow, 144 pp. (in Russian).
- Spektor, V.B., Spektor, V.V., Bakulina, N.T., 2011. Buried snowfields on the Lena-Amga plain. *Earth’s Cryosphere XV* (4), 16–21.
- Spektor, V.B., Spektor, V.V., Torgovkin, Ya.I., et al., 2016. Areal hydrogenic forms and associated floodstreams on the territory of the Central Yakut Plain at the turn of the Pleistocene and Holocene. In: *Geography Issues. Vol. 142 Geography of the polar regions*. Kodeks, Moscow, pp. 291–315 (in Russian).
- Spektor, V.V., Spektor, V.B., Boeskorov, G.G., et al., 2017. Periglacial alluvium of the Central Yakut Plain according to the study of the reference outcrop Sand Hill. *Vestnik ZabGU* [Bulletin of Trans-Baikal State University], 23 (5), 45–59.
- Ufimtsev, G.F., Dzhannota, A., Perevalov, A.V., et al., 1997. Aeolian landscapes of the Tunkinskaya depression. *Geografiya i prirodnye resursy* [Geography and Natural Resources], No. 1, 65–70.
- Velichko, A.A., Timireva, S.N., 2005. Western Siberia – the great late glacial desert. *Priroda* [Nature], No. 5, 54–62.
- Volkov, I.A., 1971. Late Quaternary subaerial formation. *Nauka*, Moscow, 274 pp. (in Russian).
- Vyrkin, V.B., 2010. Aeolian relief formation in the Baikal and Transbaikalian regions. *Geografiya i prirodnye resursy* [Geography and Natural Resources], No. 3, 25–32.
- Waters, M.R., Forman, S.L., Pierson, J.M., 1999. Late quaternary geology and geochronology of Diring an early Paleolithic site in Central Siberia. *Quaternary Research*, No. 51, 195–211.
- Wolfe, S., Bond, J., Lamothe, M., 2011. Dune stabilization in central and southern Yukon in relation to early Holocene environmental change, northwestern North America. *Quaternary Science Reviews*, No. 30 (3–4), 324–334.
- Zieliński, P., Sokołowski, R., Woronko, B., Jankowski, M., Fedorowicz, S., Zaleski, I., Molodkov, A., Weckwerth, P., 2015. The depositional conditions of the fluvio-aeolian succession during the last climate minimum based on the examples from Poland and NW Ukraine. *Quaternary International* 386, 30–41.
- Zykina, V.S., Zykin, V.S., Volvach, A.O., et al., 2017. Upper quaternary deposits of the Nadym Ob area: stratigraphy, cryogenic formations, and deposition environments. *Earth’s Cryosphere XXI* (6), 12–20.

*Received June 4, 2020*

*Revised version received August 2, 2020*

*Accepted November 25, 2020*